frontiers | Frontiers in Amphibian and Reptile Science

TYPE Original Research
PUBLISHED 02 July 2024
DOI 10.3389/famrs.2024.1411516

OPEN ACCESS

EDITED BY
Jenna M. Crowe-Riddell,
La Trobe University, Australia

REVIEWED BY
Hugues-Alexandre Blain,
Institut Català de Paleoecologia Humana i Evolució Social (IPHES), Spain
Belen von Baczko,
National Scientific and Technical Research Council (CONICET), Argentina
Duncan Leitch,
University of California, Los Angeles, United States

*CORRESPONDENCE
Emily J. Lessner
ejlessner@gmail.com

RECEIVED 03 April 2024
ACCEPTED 27 May 2024
PUBLISHED 02 July 2024

CITATION
Lessner EJ, Xu X, Young BA, Echols MS, Jones MEH, Elsey RM and Holliday CM (2024) Predicting behavior in extinct reptiles from quantitative analysis of trigeminal osteological correlates.
Front. Amphib. Reptile Sci. 2:1411516.
doi: 10.3389/famrs.2024.1411516

Predicting behavior in extinct reptiles from quantitative analysis of trigeminal osteological correlates

Emily J. Lessner[1,2]*, Xing Xu[3,4], Bruce A. Young[5], M. Scott Echols[6,7], Marc E. H. Jones[8,9], Ruth M. Elsey[10] and Casey M. Holliday[1]

[1]Department of Pathology and Anatomical Sciences, University of Missouri, Columbia, MO, United States, [2]Bureau of Land Management, Moab, UT, United States, [3]Centre for Vertebrate Evolutionary Biology, Yunnan University, Kunming, China, [4]Institute of Vertebrate Paleontology and Paleoanthropology, Chinese Academy of Sciences, Beijing, China, [5]Department of Anatomy, Kirksville College of Osteopathic Medicine, Kirksville, MO, United States, [6]Medical Center for Birds, Oakley, CA, United States, [7]Scarlet Imaging, Murray, UT, United States, [8]Science Group: Fossil Reptiles, Amphibians and Birds Section, Natural History Museum London, London, United Kingdom, [9]School of Biological Sciences, University of Adelaide, Adelaide, SA, Australia, [10]Louisiana Department of Wildlife and Fisheries, Rockefeller Wildlife Refuge, Grand Chenier, LA, United States

Introduction: Vertebrate sensory systems are in close contact with surrounding tissues, often leaving bony signatures behind. These bony features are the keys to assessing variation in sensory systems in fossil taxa. The trigeminal sensory system (e.g., trigeminal ganglion, ophthalmic, maxillary, and mandibular divisions) has osteological correlates throughout the skull, including the braincase (e.g., trigeminal fossa, prootic notch, ophthalmic and maxillomandibular foramina) and rostrum (e.g., mandibular canal, neurovascular foramina).

Methods: Here we measured and compared these features among a morphologically, phylogenetically, and ecologically diverse sample of sauropsids to determine strength of osteological correlates and to explore ecomorphological trends. We determined several suitable osteological correlates for trigeminal soft tissue features and discounted foramen count alone as a suitable osteological correlate. However, when size was accounted for, foramen count becomes a useful indicator of sensory ecology.

Results and discussion: Among extant taxa, those engaging in tactile sensory behaviors with the face exhibit relatively larger trigeminal tissues and osteological correlates than those not engaging in tactile sensory behaviors. Though patterns are unclear among several clades, both relative feature sizes and models used to predict sensory capacity reveal a trend of increasing tactile sensitivity along the pseudosuchian lineage. Overall, a quantitative assessment of ecomorphological trends of trigeminal osteological correlates proves informative for the hypotheses of sensory behavior in extinct taxa and supports the use of similar assessment methods for other osteological correlates.

KEYWORDS

sauropsid, ecomorphology, somatosensation, sensory ecology, paleontology

1 Introduction

Descriptive and qualitative variations in the trigeminal nervous system and osteological correlates are well known among sauropsids (i.e., the clade containing lepidosaurs, turtles, crocodylians, and avians). This morphological variation is associated with the tactile sensory capabilities of the rostrum as these taxa engage in feeding behaviors; some reptiles exhibit enhanced sensory abilities (e.g., crocodylians, Leitch and Catania, 2012; dabbling and probing birds, Cunningham et al., 2013), whereas others engage in behaviors requiring less tactile sensory ability (e.g., lizards and other birds). However, minimal quantitative and comparative assessment of the relevant features and behaviors has been performed (e.g., Lessner et al., 2023a), and the few assessments have explored only small clades of reptiles or single cranial features (e.g., Iwaniuk et al., 2009; George and Holliday, 2013). This project aims to expand the knowledge of trigeminal features and increase the predictive power of osteological correlates in predicting the somatosensory behaviors of extinct organisms. Particularly, rarely have ecological categorizations of taxa been used in the quantitative comparison of trigeminal osteological features (e.g., Wylie et al., 2015; Lessner et al., 2023a).

1.1 Trigeminal nerve anatomy and osteological correlates among sauropsids

The conserved trigeminal soft tissue anatomy of sauropsids is well known (see Holliday and Witmer, 2007; Lessner et al., 2023a for review). The fifth and primary somatosensory cranial nerve originates from the hindbrain, comprises one or two ganglia, and collects three divisions that innervate the face (i.e., ophthalmic, maxillary, and mandibular), all co-occurring with osteological correlates.

Among sauropsids, the surrounding bone differs with respect to the trigeminal ganglion and divisions. In lepidosaurs, the trigeminal ganglion sits within the trigeminal notch of the prootic bone just ventral to the prootic-epipterygoid suture (Figure 1; Oelrich, 1956;

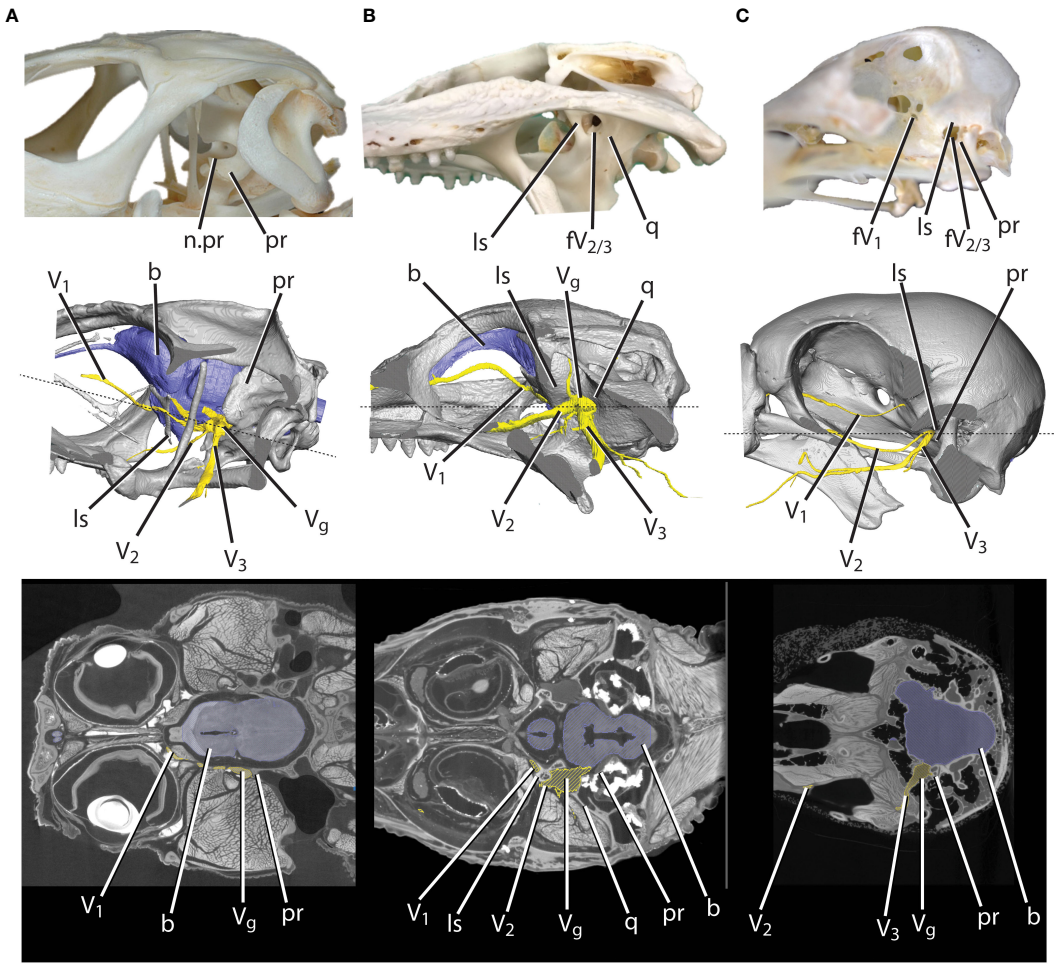

FIGURE 1
Skull cutaways of **(A)** lizard, **(B)** alligator, and **(C)** bird featuring bony features, 3D-modeled skull from iodine data with brain and nerves, and CT slice data. b, brain; fV_1, foramen for the ophthalmic division of the trigeminal nerve; $fV_{2/3}$, foramen for the maxillomandibular divisions of the trigeminal nerve; ls, laterosphenoid; n.pr, prootic notch; pr, prootic; q, quadrate; V_1, ophthalmic division of the trigeminal nerve; V_2, maxillary division of the trigeminal nerve; V_3, mandibular division of the trigeminal nerve; V_g, trigeminal ganglion.

Barbas-Henry and Lohman, 1986). In most lepidosaurs, the trigeminal notch is only bounded rostrally by a tendinous ligament, creating a single foramen for the three trigeminal divisions (Oelrich, 1956; Evans, 2008). In pseudosuchians, the trigeminal ganglion is housed extracranially in the trigeminal fossa, a bony cavity lateral to the braincase formed by the quadrate, prootic, laterosphenoid, and pterygoid (Hopson, 1979; Witmer et al., 2008; Holliday and Witmer, 2009) (Figure 1). Therefore, in pseudosuchians, a trigeminal foramen in the braincase allows the transmission of the trigeminal nerve into the trigeminal fossa and the three divisions pass through the bony foramina in their exit from the trigeminal fossa. The pseudosuchian ophthalmic division exits the ganglion rostrally via a foramen in the laterosphenoid, whereas the pseudosuchian maxillary and mandibular divisions exit the trigeminal ganglion laterally through the maxillomandibular foramen, bounded by the laterosphenoid and prootic (Jollie, 1962; Holliday and Witmer, 2009) (Figure 1). Trigeminal ganglion and division foramina are more variable in avemetatarsalians. In sauropod dinosaurs, there is a single trigeminal foramen, indicating an extracranial (though not surrounded by bone) trigeminal ganglion (Hopson, 1979; Holliday, 2009; Balanoff et al., 2010). This pattern contrasts with more derived avian-line condition in which the trigeminal ganglion is found within the braincase (Holliday, 2006; Witmer et al., 2008). This intracranial placement is reflected by the presence of separate ophthalmic and maxillomandibular foramina within the braincase wall of many tetanuran dinosaurs (Witmer and Ridgely 2009). In extant birds, the trigeminal ganglion (occasionally partially divided) is located on the floor of the cranial cavity (Baumel and Witmer, 1993). In avian-line archosaurs with an intracranial ganglion, the ophthalmic division exits the braincase through a foramen between the laterosphenoid and basicranium (e.g., basisphenoid, parasphenoid, ethmoid), and the maxillary and mandibular divisions typically exit the braincase through the maxillomandibular foramen, bounded by the laterosphenoid and prootic (though some birds have separate maxillary and mandibular foramina) (Baumel and Witmer, 1993) (Figure 1). In addition to transmitting sensory signals from the mandibles, the mandibular division transmits motor signals to the musculature of the lower jaw. Because the ophthalmic and maxillary divisions transmit signals from a complex range of origins across the face (e.g., nasal and oral cavities, orbit, sclera, palate, upper jaw), the osteological correlates for these nerves are more complicated in interpretation. The mandibular division's limited innervation pattern (e.g., jaw muscles, lower jaw, tongue, teeth) means that the interpretation of osteological correlates is less complicated, and therefore we chose to focus on the osteological correlates of this division.

Motor branches from the mandibular nerve originate proximally near the trigeminal foramen and innervate jaw muscle compartments via the internal constrictor, pterygoid, temporal, and caudal rami; the branch for the anterior intermandibularis muscle originates just proximal to the mandibular nerve's entry into the mandible (Holliday and Witmer, 2007; Abdel-Kader et al., 2011; Watkinson, 1906; Lakjer, 1926; Poglayen-Neuwall, 1953; Watanabe and Yasuda, 1970; Schumacher, 1973). Proximal sensory branches from the mandibular division include the anguli oris nerve to the corner of the mouth and the recurrent cutaneous nerve to the skin over the adductor mandibularis externus. Further distally, the mandibular division extends the large caudal intermandibular or external cutaneous branch medially through the angular, which sends numerous cutaneous rami to the skin of the ventrolateral mandible. As the mandibular nerve enters the mandibles, medial and oral intermandibular branches extend to innervate the epithelium of the mouth, dental lamina, and integument and the inferior alveolar nerve enters the dentary (Abdel-Kader et al., 2011; Poglayen-Neuwall, 1953; Watanabe and Yasuda, 1970; Holliday and Witmer, 2007; Lessner et al., 2023a). Numerous lingual, mucosal, and dental branches extend from the intermandibular and inferior alveolar nerves to their terminations in the oral cavity, and the foramina in the dentary transmits cutaneous branches to their terminations in the integument of the rostral mandibles. Afferent terminations of the trigeminal nerve include both free nerve endings and sensory structures that are mostly mechanosensitive in function (e.g., Hiller, 1978; Berkhoudt, 1980; Baumel and Witmer, 1993; Cunningham et al., 2010; Goris, 2011; Di-Poï and Milinkovitch, 2013).

1.2 Osteological correlates and inferring sensation

Osteological correlates and knowledge of taxa with enhanced trigeminal sensory abilities within the extant phylogenetic bracket of lepidosaurs, crocodylians, and birds indicate the potential for specialized trigeminal nerve-innervated sensation in additional members of Archosauria (as per Witmer and Thomason, 1995). Taxa exhibiting enhanced trigeminal somatosensitive abilities or specializations are generally known, having been observed to engage in distinct behaviors. Among sauropsids, these include extant crocodylians, known for their abilities to discriminate between fine stimuli in the semi-aquatic environment (e.g., Leitch and Catania, 2012; Di-Poï and Milinkovitch, 2013; Grap et al., 2020). Other specialized somatosensitive taxa are probing and dabbling birds, which make use of tactile cues to acquire food particles and prey (e.g., Gottschaldt and Lausmann, 1974; Cunningham et al., 2010, 2013). Generally, with the exception of some snakes (e.g., Catania et al., 2010; Goris, 2011; Crowe-Riddell et al., 2019), lepidosaurs are assumed to engage in minimal trigeminal-innervated somatosensory behaviors, though their specific ecologies remain unknown.

Witmer and Thomason (1995) demonstrated that soft tissue inference is necessary for forming hypotheses on functional morphology, behavior, ecology, and evolution and noted the importance of basing soft tissue inferences in extant organisms on osteological data acquired from a sample of extant organisms. As such, there are multiple examples of research examining osteological structures as correlates for neural soft tissues to make further inferences of behavior and ecology (e.g., Muchlinski, 2008; Bird et al., 2014, 2018). Because a nerve cross-sectional area may be used to estimate axon counts (Jonas et al., 1992; Mackinnon and Dellon, 1995; Cull et al., 2003), regions with high densities of sensory receptors require more innervation (Kandel et al., 2000;

Oelschlager and Oelschlager, 2002; Marino, 2007), and regions with higher receptor densities exhibit higher sensitivities (Dehnhardt and Kaminski, 1995; Nicolelis et al., 1997), it is possible to estimate the nerve cross-sectional area, axon count, and sensitivity of the region innervated all from the relevant osteological correlates.

Previous evolutionary studies of the sauropsid trigeminal system have mostly focused on pseudosuchians, the sister clade to bird-line archosaurs (e.g., Soares, 2002; George and Holliday, 2013; Lessner, 2021; Lessner et al., 2023a). Though extant crocodylians are conservative in morphology and ecology, occupying similar semi-aquatic niches, extinct pseudosuchians exhibited diverse forms and occupied terrestrial to aquatic habitats, navigating these environments with unknown sensory abilities. Soares (2002) began with an investigation into the trigeminal system in crocodylians, discovering that the sensory organs were receptive to pressure changes and hypothesizing that the foraminiferous jaws representative of this system were only present in semiaquatic members present after the Early Jurassic. George and Holliday (2013) performed quantitative analyses, establishing that *Alligator mississippiensis* head length, brain size, and trigeminal nerve size are consistently related. This confirmed the trigeminal ganglion size as an informative metric for trigeminal nerve size in crocodyliforms and as an informative proxy for sensitivity, leading to the hypothesis that the unique system seen in extant crocodylians likely originated along the eusuchian line. Lessner et al. (2023a) demonstrated a stepwise progression of mandibular nerve complexity among crocodylians and inferred an increase in sensory abilities among pseudosuchians that preceded their ecological transition from the terrestrial to semiaquatic habitat.

Recent studies have applied these osteological correlates to avian-line archosaurs, both terrestrial and aquatic, inferring sensitivity based on the presence of foramina. The presence of neurovascular foramina is cited within Dinosauria as a proxy for trigeminal nerve-innervated sensitivity (Ibrahim et al., 2014; Barker et al., 2017; Rothschild and Naples, 2017, etc.). However, these hypotheses remain qualitative, were based on the presence or absence of foramina and canals, and have not been supported by quantitative analyses of the associated trigeminal ganglia and osteological correlates, neurovascular canals, or rostral foramina.

Here we assess the strength of trigeminal osteological correlates, use what knowledge exists in the literature to determine whether there is a relationship between correlate size and ecology, and make predictions in fossil taxa based on these results. The resulting predictions are used to inform evolutionary trends in trigeminal-innervated somatosensory behaviors.

2 Materials and methods

2.1 Specimens

Both osteological and digital specimens were investigated for this project (see Supplementary File S1 for all specimens). Some extant specimens underwent iodine contrast-enhanced microCT scanning (Gignac et al., 2016) to enhance the contrast between hard and soft tissue structures. Other extant and all fossil specimens underwent conventional micro- and medical CT scanning to differentiate bone from surrounding tissue, matrix, or air.

2.2 Measurements

From extant, contrast-enhanced CT-scanned specimens, data on the volume of the trigeminal ganglion and cross-sectional area and height of the mandibular division of the trigeminal nerve at the proximal opening of the mandibular canal were collected. Data on osteological features (i.e., skull width, length, and height, foramen magnum width, trigeminal fossa volume, maxillomandibular foramen diameter, mandibular nerve foramen cross-sectional area and height, rostral dentary foramen count, rostral dentary length, rostral dentary surface area) were collected from all extant contrast-enhanced specimens, from additional extant specimens, and from various fossil specimens. The trigeminal fossa was measured as the space bounded by the laterosphenoid, prootic, and quadrate. Data on both the maximum and the minimum distance across the foramen through which the maxillary and mandibular (and sometimes ophthalmic) division pass were collected.

We focused on the mandibular division of the trigeminal nerve because its sensory targets are largely integumentary, providing the best signal for inferences of sensory behaviors from osteological correlates. Data on the cross-sectional area and height of the mandibular nerve were collected at the proximal-most extent of the mandibular canal, at the first instance where the canal exhibited a complete enclosure. This point is rostral to the separation of the lingual branch of the trigeminal nerve, and thus measurements are not in conflict with any influence of tongue innervation requirements (Lessner et al., 2023a). The dentary measurements (i.e., foramen count, length, surface area) were taken rostral to the proximal opening of the mandibular canal. The dentary surface area only included the lateral, integumentary surface of the dentary. Additional dimensions were measured, (i.e., skull width, length, and height, foramen magnum width), and data were collected as proxies toward normalizing for body size.

Soft tissue features were measured digitally using a 3D-imaging software, Avizo (Thermo Fisher Scientific; Waltham, MA). Linear measurements were collected using the "Measure: 2D length" tool, and data on cross-sectional areas were collected using the "Material Statistics: Area per slice" module. Details on surface areas were collected using the surface editor and "Surface Area Statistics" module. The trigeminal ganglia, trigeminal fossae, and mandibular canals were manually segmented and verified in three planes using magic wand and paint-brush tools with interpolation. Volumes were collected using the "Material Statistics" module.

2.3 Analysis

The abovementioned measurements were compared to determine the statistical significance of osteological correlates and to test for shared morphological patterns within ecological groups. Correlation was assessed while accounting for phylogeny using the R package "phytools" (Revell, 2012). Proxies for size were

determined based on correlation with skull volume (calculated from length, diameter, and width as elliptical cylinders; Hurlburt, 1999). Because of the damaged or partial nature of many specimens, we determined the utility of the foramen magnum width and anterior dentary surface area using phylogenetic linear modeling (Revell, 2012) and the R packages "ape" (Paradis and Schliep, 2019), "nlme" (Pinhiero et al., 2013), and "phytools" (Revell, 2012). Based upon observed behaviors from the literature (Leitch and Catania, 2012; Cunningham et al., 2013; Di-Poï and Milinkovitch, 2013; Grap et al., 2020), each extant specimen was assigned to one of two groups or ecologies: those engaging in tactile sensory behaviors and those in which tactile sensory behaviors were absent (Supplementary File S1). Group differences were tested for all variables in R using the "evomap" (Smaers and Mongle, 2014) package to run phylogenetic ANCOVAs. Generalized linear models (i.e., discriminant analysis) were used to estimate probabilities to decide group membership for fossil specimens using R packages "stats" (R Core Team, 2021) and "MASS" (Venables and Ripley, 2002). The R package "mice" (van Buuren and Groothuis-Oudshoorn, 2011) was used for imputing data. The phylogeny used in the analysis was adapted from those listed in Supplementary File S2 (see Supplementary File S3 for phylogeny). Multiple specimens per species were represented as hard polytomies, and branch lengths were estimated using the R packages (phytools) (Revell, 2012) and "geiger" (Pennell et al., 2014) to calculate and assign Pagel's lambda per variable (Pagel, 1999). Significance was assessed at an alpha level of $p = 0.05$.

3 Results

3.1 Gross anatomy

This section expands on the description of the osteological correlates of the mandibular nerve provided by Lessner et al. (Lessner, 2022; Lessner et al., 2023a) by adding a description of turtles and additional fossil specimens (Figure 2). Archosaurs and other reptiles show a diversity of morphological patterns in how the trigeminal ganglion and divisions interact with the lateral braincase wall (e.g., Oelrich, 1956; Jollie, 1962; Hopson, 1979; Barbas-Henry and Lohman, 1986; Holliday, 2006; Evans, 2008; Witmer et al., 2008; Holliday, 2009; Holliday and Witmer, 2009; Balanoff et al., 2010; Witmer and Ridgely 2009; Baumel and Witmer, 1993; Goris, 2011; Dollman, 2020). For this analysis, we will forego an anatomical description of this morphology and focus on measurements of fossae and foramina used in this morphometric analysis of nerve function.

Among sauropsids, the dentary is the main and rostralmost bone of the lower jaw and bears the fossae and formina studied here. Here we detail the descriptions of osteological correlates of trigeminal tissues in the dentary (e.g., mandibular canal, lateral foramina) made from direct observation of fossil material of various sauropsids. Several observations apply to all taxa, including the foramina on the caudal portion of the dentary that are often groove-like, and the grooves are directed caudally; if the specimen possesses a rostral mandible that is mediolaterally wide rather than dorsoventrally tall, there is a concentration of rostral foramina; and there is a row of foramina paralleling the dorsal dentary margin. In the descriptions below, "few" describes foramina counts typically less than 30, but density is based on mandible surface area, which was not quantified for all taxa [see Lessner et al. (2023a) for an analysis of density].

Turtles are unique in the possession of densely perforated, edentulous, rhampthotheca-covered mandibles. *Caretta* (TMM M-7143) and *Chelydra* (TMM M-2337) possess highly perforated dentaries, *Trachemys* (TMM M-858, 7159) has slightly less perforated dentaries, and *Gopherus* (TMM M-4934) and *Trionyx* (TMM M-3132) have even less perforated dentaries. All have a distinctive row of foramina along the tomial edge of the dentary. *Gopherus* (TMM M-4934) possesses a rostral concentration of foramina, and the pattern in *Caretta* (TMM M-7143) is radiate, resembling that of aetosaurs (extinct pseudosuchians).

The neodiapsid *Champsosaurus* (YPM 16239) has few foramina (approximately eight) on the dentary; most of those present are located along the alveolar margin and are elongate and groove-like in shape. This is similar to the condition in lepidosaurs [see Lessner et al. (Lessner, 2022; Lessner et al., 2023a) for more description] in which there tends to be five to six foramina distributed in a line paralleling the tooth row (Figure 3A). The allokotosaurid archosauromorph *Trilophosaurus* (TMM 31025–125, 116, 223) has a similar arrangement in which there are few foramina present (~19), with most falling in a row parallel to the alveolar margin (Figure 3B). The mandibular canal in *Trilophosaurus* (TMM 31025–233) becomes distinct from the Meckelian fossa at the level of the 7th tooth (from rostral) and is located ventromedial to the teeth. The archosauriform *Proterochampsa* (MCZ 3408) possesses a higher density of foramina, which are elongate in shape.

Among crocodylian-line archosaurs, phytosaurs *Mystriosuchus* (SMNS 9134), *Rutiodon* (YPM 7899), and the unidentified MNA V3601 have a higher density of foramina than the non-archosaur diapsids and a row of foramina paralleling the tooth row. Phytosaurs typically possess a rostral concentration of foramina on the dentary tip. The mandibular canal in phytosaurs (MNA V3601) is located lateral to the alveoli rostrally. Aetosaurs *Paratypoyhorax* (SMNS 19003), *Stenomyti* (DMNH 60708), *Aetosaurus* (SMNS 5770), and *Longosuchus* (TMM 31100–1338, TMM 31185–84) have a low density of foramina (approximately eight to 34) that are accompanied by grooves arranged in a stellate pattern, radiating from a point on the rostrolateral surface of the mandible (Figure 3C). Aetosaurs also possess a row of foramina on the edentulous portions of the mandible and paralleling the alveolar margin. A foramen is present at the rostral tip of the mandible. The mandibular canal in *Longosuchus* (TMM 31185–84) becomes distinct from the dorsal aspect of the Meckelian fossa at the level of the fourth tooth (from rostral) and continues rostrally lateral to the alveoli. The non-paracrocodylomorph suchian *Gracilisuchus* (MCZ 4117), as well as the unnamed suchian SMNS 1977, and the non-crocodylomorph loricatans *Saurosuchus* (MCZ 4687, 4690) and *Batrachotomus* (SMNS 52970, 80260) all have few foramina (approximately four to 27). In *Batrachotomus* (SMNS 52970, 80260), there is a distinct line of foramina within a groove paralleling the alveolar margin caudally and the alveolar margin

10.3389/famrs.2024.1411516

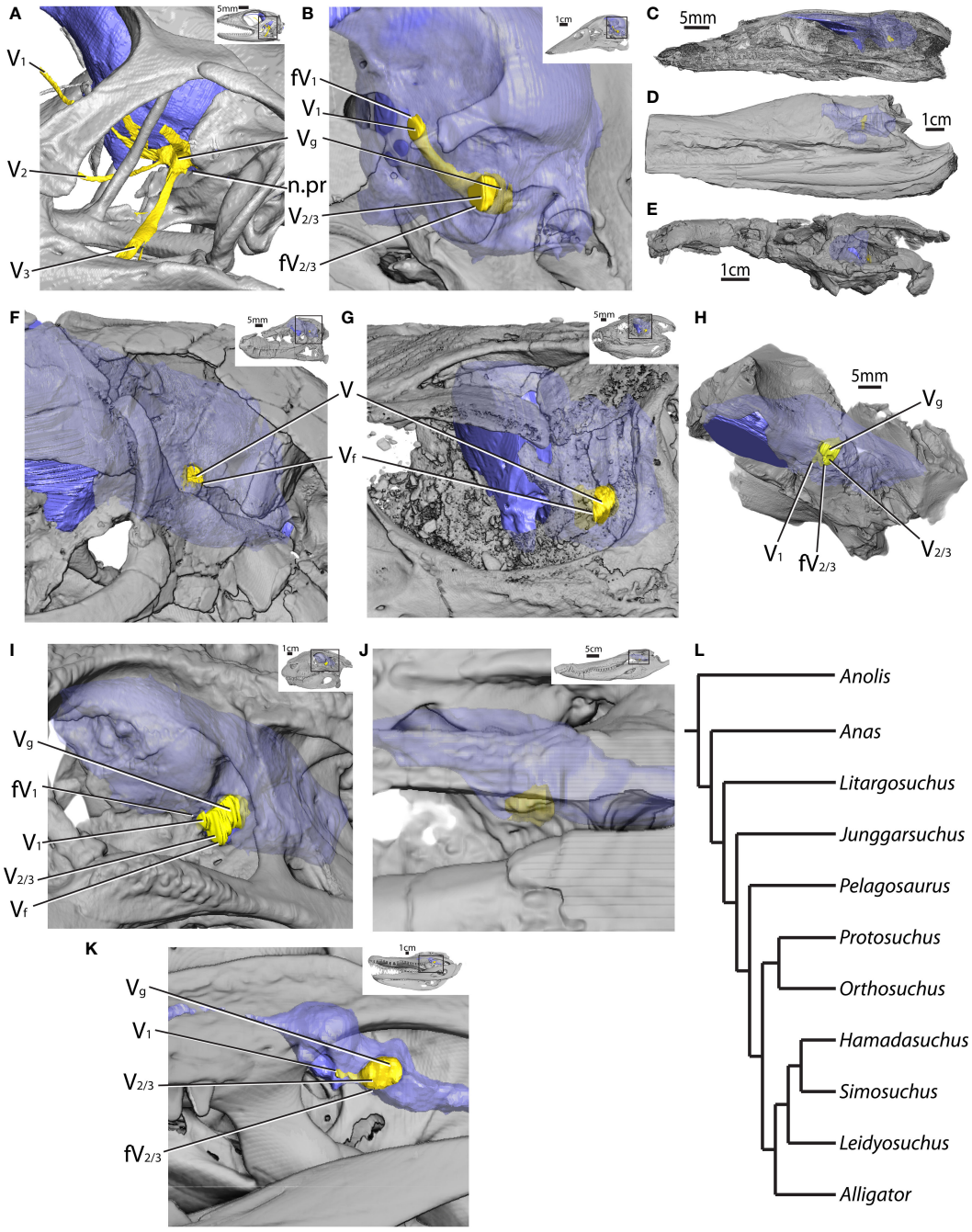

FIGURE 2
Lateral braincases of selected CT-scanned taxa with reconstructed endocasts (blue) and trigeminal ganglia and nerves (yellow) in **(A)** *Anolis* (MUVC LI089; reflected), **(B)** *Anas* (OUVC 10252; reflected), **(C)** *Litargosuchus* (BP 5237; reflected), **(D)** *Pelagosaurus* (BRLSI M1413), **(E)** *Orthosuchus* (SAM PK K409; reflected), **(F)** *Junggarsuchus* (IVPP V14010), **(G)** *Protosuchus* (BP I 4770; reflected), **(H)** *Hamadasuchus* (ROM 54513), **(I)** *Simosuchus* (UA 8679), **(J)** *Leidyosuchus* (ROM 1903), **(K)** *Alligator* (MUVC AL606, reflected), and **(L)** phylogeny of figured taxa. fV_1, foramen for the ophthalmic division of the trigeminal nerve; $fV_{2/3}$, foramen for the maxillomandibular divisions of the trigeminal nerve; n.pr, prootic notch; V, trigeminal nerve; V_1, ophthalmic division of the trigeminal nerve; V_2, maxillary division of the trigeminal nerve; V_3, mandibular division of the trigeminal nerve; V_f, trigeminal foramen; V_g, trigeminal ganglion.

rostrally. SMNS 80260 also has a distinct row of foramina along the ventral margin of the dentary, and the opening for the mandibular canal is present at the rostral narrowing of the Meckelian fossa. In the non-crocodyliform crocodylomorphs *Litargosuchus* (BP 5237), *Junggarsuchus* (IVPP V14010), and the unnamed YPM 57103, there is a low density of foramina with a row of foramina paralleling the alveolar and ventral dentary margins (~26–34) (Figures 3D, F). In the non-crocodyliform crocodylomorph *Macelognathus* (LACM 150148), there is a higher density of foramina especially at the rostral edentulous portion of the jaw (~30) (Figure 3E). In *Litargosuchus* (BP 5237), *Junggarsuchus* (IVPP V14010), and *Macelognathus*, (LACM 150148), the mandibular canal is located

10.3389/famrs.2024.1411516

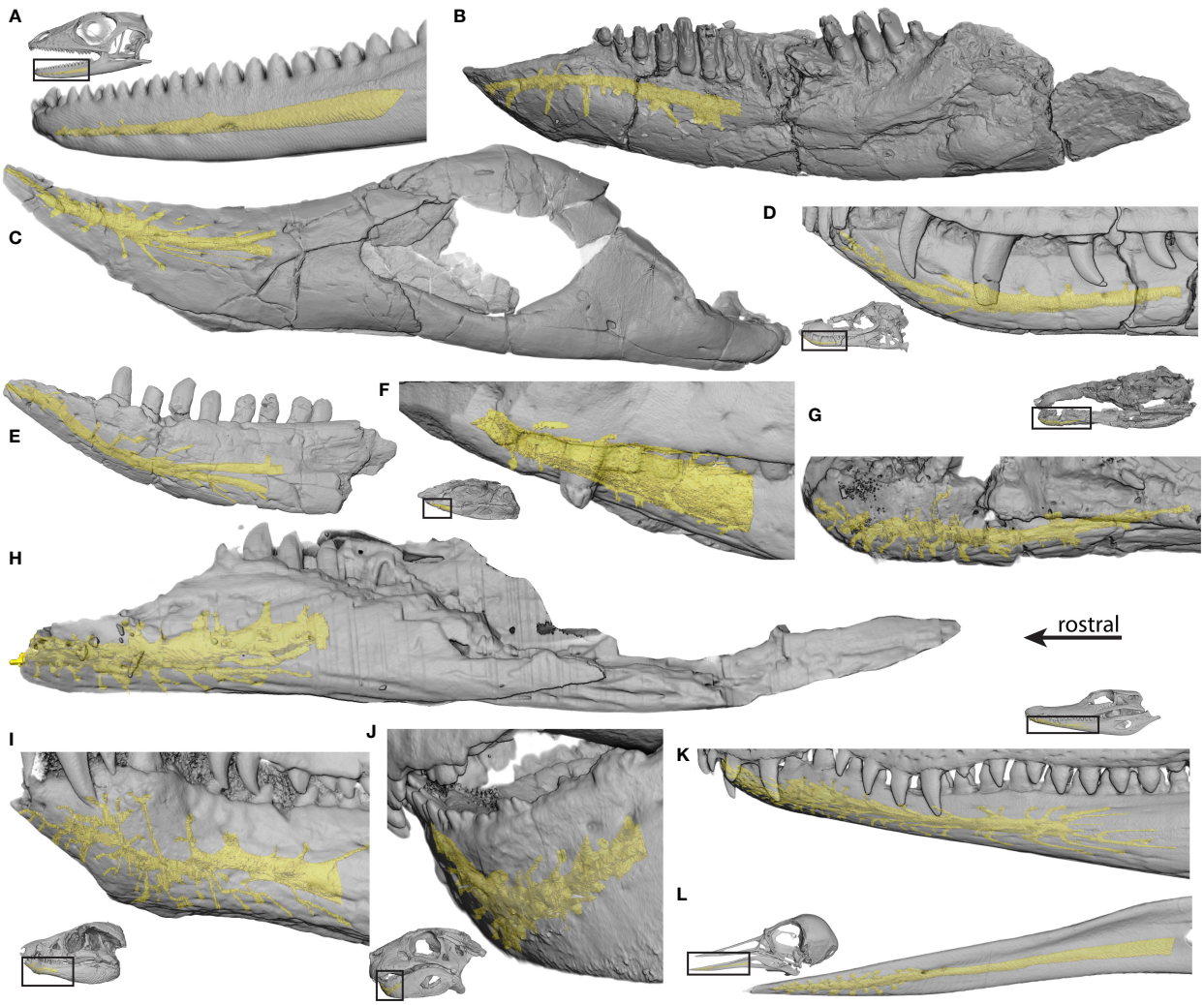

FIGURE 3
Dentaries of selected CT-scanned taxa with reconstructed mandibular neurovascular canals (yellow) in **(A)** *Anolis* (MUVC LI089, reflected), **(B)** *Trilophosaurus* (TMM 31025–233, reflected), **(C)** *Longosuchus* (TMM 31185–84), **(D)** *Junggarsuchus* (IVPP V14010), **(E)** *Macelognathus* (LACM 150148), **(F)** *Nominosuchus* (IVPP 14392), **(G)** *Orthosuchus* (SAM PK K409, reflected), **(H)** *Araripesuchus* (AMNH 24450), **(I)** *Protosuchus* (BP I 4770), **(J)** *Simosuchus* (UA 8679, reflected), **(K)** *Caiman* (FMNH 73711, reflected), and **(L)** *Arenaria* (USNM 612977).

ventrolateral to the alveoli. The protosuchian crocodylomorph *Platyognathus* (CUP 2083) has a large opening for the mandibular canal. Several thalattosuchians were investigated, including *Steneosaurus* (SMNS 53661, 20218, 10114; P 14541), *Machimosaurus* (SMNS 81608, 91415), *Pelagosaurus* (SMNS 50374; BRSLI M1413), *Metriorhynchus* (SMNS 10115), and *Dakosaurus* (SMNS 8203), all of which possessed a low density of foramina (~38). The foramina of the thalattosuchians were elongate and groove-like. In *Dakosaurus* (SMNS 8203), the foramina paralleled the tooth row and the ventral dentary margin, and in *Machimosaurus* (SMNS 91415), there was a rostral concentration of foramina. The non-neosuchian crocodyliforms *Protosuchus* (BP 1 4770; MCZ 6727), *Orthosuchus* (SAM PK K409), and *Nominosuchus* (IVPP 14392) have a higher density of foramina (~26–69) and *Protosuchus* (BP 1 4770; MCZ 6727) has a notable rostral concentration (Figures 3F, G, I). The mandibular canal in these taxa is located ventrolateral to the alveoli and is large in *Nominosuchus* (IVPP 14392). Among notosuchians, the more basal *Mahajangasuchus* (FMNH PR 2721) and *Kaprosuchus* (MNN IGU 12) have a low density of foramina but exhibit high rugosity of the mandible. In *Kaprosuchus* (MNN IGU 12), the foramina are present largely along the alveolar margin. Other notosuchians, *Simosuchus* (UA 8679), *Anatosuchus* (MNN GAD17), and *Araripesuchus* (MNN GAD20, 27; UCRCPV 3; AMNH 24450) possess more foramina (~35–40) exhibiting high rostral densities, with lower densities elsewhere across the dentary (Figures 3H, J). In *Simosuchus* (UA 8679) and *Araripesuchus* (AMNH 24450), the mandibular canal is located ventrolateral to the alveoli. The tethysuchid *Elosuchus* (UCRCPV G4–7) exhibits a low density of foramina. The unnamed non-crocodylian eusuchian MCZ 4453 has a high density of foramina, and the basal non-crocodylian eusuchian *Laganosuchus* (UCRCPV 2) has a low density of foramina. The crocodylians *Allognathosuchus* (FMNH P 12141), *Gavialosuchus* (UC 610), *Alligator mcgrewi* (FMNH P 26242), and

Alligator olseni (MCZ 4703) all exhibit density on the scale of extant crocodylians, whereas *Diplocynodon* (SMNS 59595) has fewer foramina along with a higher rugosity and elongate, narrow foramina. Extant crocodylians all share a high density of foramina with a rostral concentration (Figure 3K).

Avian mandibles (e.g., Figure 3L) are variable, and foramen distribution is associated with feeding and sensory ecology (Lessner et al., 2023a).

3.2 Confirming osteological correlates

Trigeminal ganglion volume was compared with the maximum and minimum diameters of the maxillomandibular foramen (or prootic notch in lepidosaurs) in extant reptiles while accounting for phylogeny (Table 1; Figures 4A, B). Among all reptiles, these features are highly correlated (c = 0.94). Maxillomandibular foramen diameter is even more highly correlated with trigeminal ganglion volume within crocodylians and lepidosaurs individually, though less so in birds (c = 0.95, 0.98, c = 0.96, c = 0.59, 0.61, respectively).

The cross-sectional area of the mandibular division of the trigeminal nerve as it passes into the dentary was also compared to the cross-sectional area of the mandibular canal at the same location in extant reptiles while accounting for phylogeny (Table 1; Figure 4C). Among all reptiles, these features are well correlated (c = 0.911). Correlation is stronger when assessed within crocodylians (c = 0.985) but less so when assessed just within lepidosaurs and birds (c = 0.882, 0.853, respectively).

The height of the mandibular division of the trigeminal nerve as it passes into the dentary was also compared to the height of the mandibular canal at the same location in extant reptiles while accounting for phylogeny (Table 1; Figure 4D). Among all reptiles, these features are well correlated (c = 0.868). Correlation is stronger when assessed within just lepidosaurs and birds (c = 0.977, 0.875, respectively) but less so when assessed within crocodylians (c = 0.815).

The same correlations above were assessed for extant members of the non-tactile and tactile groups and are still strong (Table 1).

Trigeminal ganglion volume and mandibular nerve cross-sectional area and height were also compared in extant reptiles to the number of foramina on the dentary rostral to the point where the mandibular nerve enters the dentary (typically excludes few foramina; Table 1; Figure 4E). Correlations are very weak among sauropsids (c = 0.453, 0.329, 0.352, respectively) and thus were not explored further.

3.3 Establishing a size proxy

Because of the limited availability of complete skeletons or skulls, to make the most from the collected data, we explored foramen magnum width as a proxy for size using 80 extant sauropsids with both foramen magnum width and head volume (metric representing size of the animal) measurable. Phylogenetic reduced major axis (RMA) regression of skull volume vs. foramen magnum width reveals a significant relationship between the two metrics (R^2 = 0.88, p-value = 0.000; Figure 5). Additionally, phylogenetic ANOVA revealed no significant differences in this relationship between clades. Because of the strength of this relationship, we use foramen magnum width as a covariate for size in future linear models involving features of the neurocranium (e.g., maxillomandibular foramen size).

We also explored the anterior (to the complete enclosure of the mandibular canal) surface area of the dentary as a proxy for size to be used when only dentaries are available for measurement. This was tested using the phylogenetic RMA regression of skull volume vs. anterior surface area in extant specimens. We find a significant relationship between the two metrics (R^2 = 0.91, p-value = 0.000; Figure 5) using 57 extant sauropsids. Additionally, phylogenetic ANOVA revealed no significant differences in this relationship between clades. We use the anterior surface area of the dentary as a covariate for size in future linear models involving mandibular features (e.g., mandibular canal size, foramen count).

TABLE 1 Correlations of soft tissue features and their osteological correlates.

Soft tissue feature	Osteological correlate	Sauropsids	Lepidosaurs	Crocodylians	Avians	Non-tactile	Tactile
Ganglion volume (mm^3)	Foramen minimum diameter (mm)	0.935	0.958	0.950	0.591	0.877	0.953
Ganglion volume (mm^3)	Foramen maximum diameter (mm)	0.943	0.960	0.985	0.609	0.827	0.975
Mandibular division cross-sectional area (mm^2)	Canal cross-sectional area (mm^2)	0.911	0.882	0.985	0.853	0.920	0.817
Mandibular division height (mm)	Canal height (mm)	0.868	0.977	0.815	0.875	0.882	0.920
Ganglion volume (mm^3)	Foramen count	0.453	–	–	–	–	–
Mandibular division cross-sectional area (mm^2)	Foramen count	0.329	–	–	–	–	–
Mandibular division height (mm)	Foramen count	0.352	–	–	–	–	–

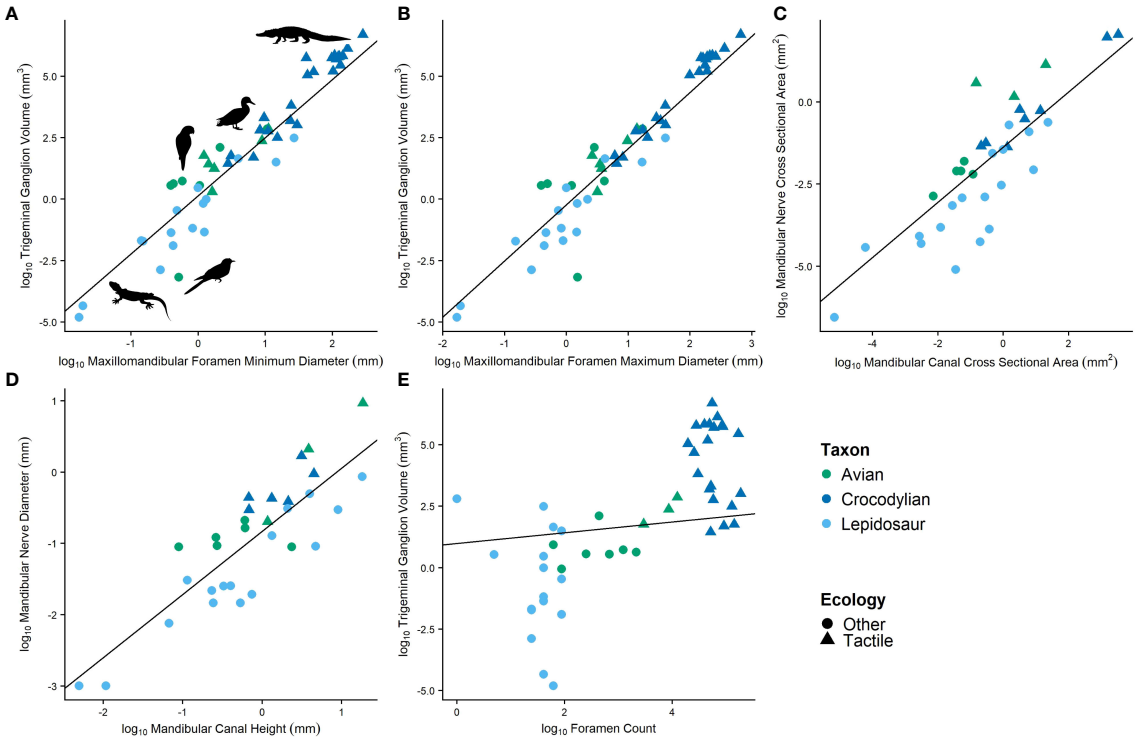

FIGURE 4
Relationships between soft tissue features and their osteological correlates featuring **(A)** trigeminal ganglion volume and minimum diameter of the maxillomandibular foramen, **(B)** trigeminal ganglion volume and maximum diameter of the maxillomandibular foramen, **(C)** cross-sectional area of the mandibular nerve and cross-sectional area of the mandibular canal, **(D)** diameter of the mandibular nerve and height of the mandibular canal, and **(E)** trigeminal ganglion volume and foramen count.

Because of the uncertainty surrounding these variables, when necessary, phylogenetic RMA regression was used to explore and illustrate (Figure 6) relationships between the proxies and other variables of interest. In this case, the size proxies are uncertain, likely covarying with unknown and unaccounted for variables, and phylogenetic RMA adjusts for this and phylogeny by assuming both the *x* and *y* variables have associated error rather than just the *y* variable.

3.4 Differences among ecologies

With osteological correlates confirmed (see "Confirming osteological correlates" above) and a proxy for size established (see "Establishing a size proxy" above), we performed phylogenetic ANCOVAs to test for size and phylogeny-controlled differences in osteological correlates among ecologies.

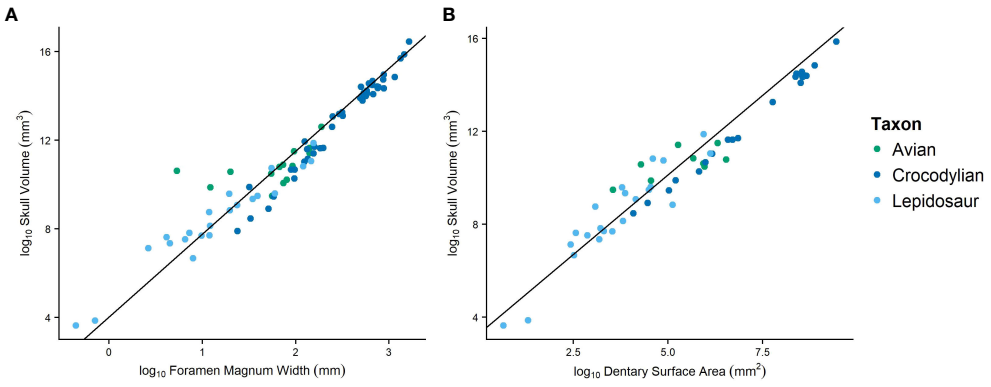

FIGURE 5
Phylogenetic RMA regression plots evaluating the foramen magnum width **(A)** and anterior dentary surface area **(B)** as proxies for body size by comparing to skull volume.

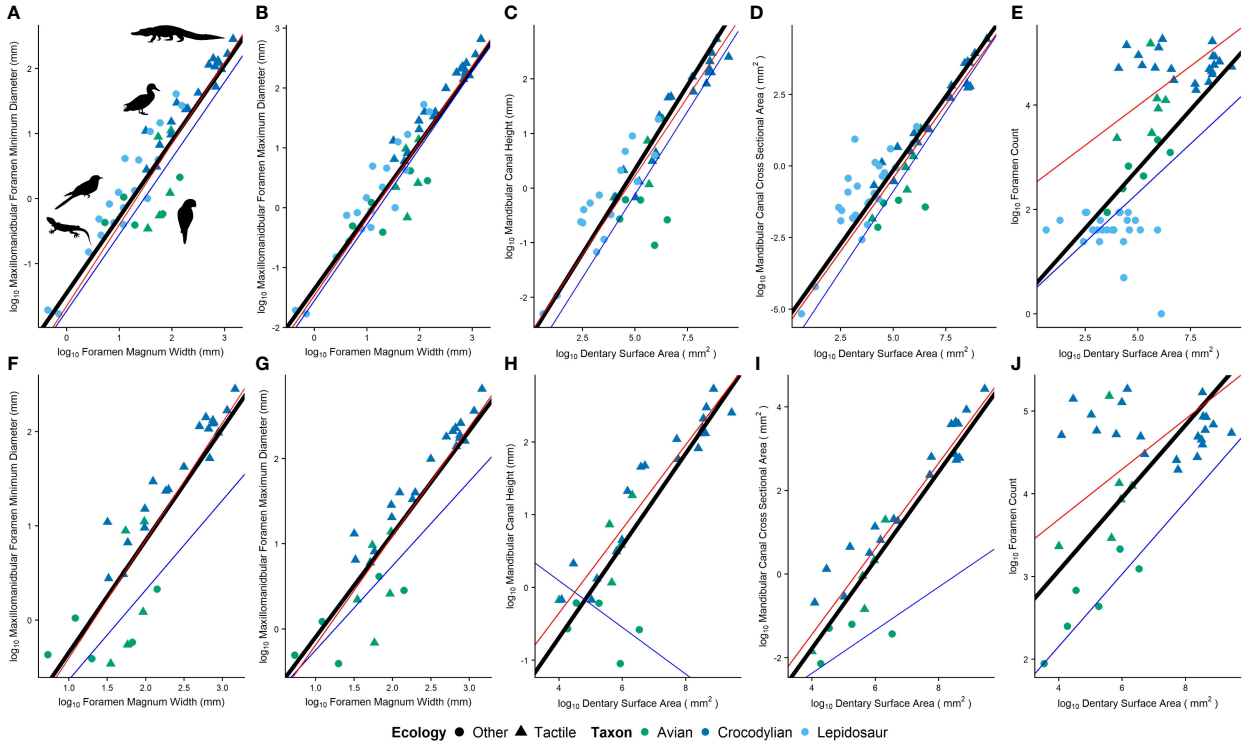

FIGURE 6
Ecological differences in relative osteological correlates including **(A, F)** minimum and **(B, G)** maximum diameter of the maxillomandibular foramen **(C, H)** cross-sectional area and **(D, I)** height of the mandibular canal, and **(E, J)** foramen count. Plots include **(A–E)** and exclude **(F–J)** lepidosaurs. The black line is a regression line calculated by phylogenetic RMA regression, the red line models the average of tactile taxa, and the blue line models the average of non-tactile taxa.

Comparisons between minimum and maximum diameters of the maxillomandibular foramen, cross-sectional area and height of the mandibular canal, and foramen count were made between tactile and non-tactile sauropsids, with size proxies included as covariates. Relative maxillomandibular foramen diameters (i.e., minimum and maximum) are not significantly different between groups (Figures 6A, B; p = 0.65, 0.90, respectively; n tactile = 53, n non-tactile = 40). Relative canal dimensions (i.e., cross-sectional area and height) are not significantly different between groups either (Figures 6C, D; p = 0.33, 0.43; n tactile = 26, 26, n non-tactile = 30, 21, respectively). Relative foramen counts are significantly different between groups (Figure 6E; $p \leq 0.0001$; n tactile = 27, n non-tactile = 32).

Since most features showed no significant differences among Sauropsida, differences were investigated within Archosauria, though this greatly reduced the sample size of non-tactile taxa. Relative maxillomandibular foramen diameters (i.e., minimum and maximum) are significantly different between groups (Figures 6F, G; p = 0.0083, 0.0023, respectively; n tactile = 53, n non-tactile = 7). Relative canal dimensions (i.e., cross-sectional area and height) and foramen counts are also significantly different between groups (Figures 6H–J; $p \leq 0.001$; n tactile = 26, 26, 27, n non-tactile = 4, 5, 6, respectively).

3.5 Predictions

With significant differences in sensory ecologies present among Archosauria, linear discriminant analysis (LDA) was used to predict the affinity of fossil specimens after removing all lepidosaurs from the dataset. For each taxon, LDA calculated posterior probabilities for sensory ecology classes (tactile vs. non-tactile); the predicted sensory class was assigned by maximum posterior probability. Additionally, LDA defined a new axis of separability on which taxa could be compared.

Of the archosaurs sampled (see Supplementary File S1), only 28 extant and seven fossil specimens had all metrics present (i.e., maxillomandibular foramen metrics, mandibular canal metrics, foramen count, size proxies). A model including all metrics predicts extant sensory ecology with 96% accuracy, with only *Psittacus* (MUVC AV092) being predicted to be opposite as classified, as a non-tactile taxon (Figure 7G). Using the rostral, mandibular metrics only, the model predicted extant sensory ecology with 97% accuracy, with only *Psittacus* (MUVC AV092) being predicted to be opposite as classified, as a non-tactile taxon (Figure 7F). Using the maximum diameter of the maxillomandibular foramen and foramen magnum width as a covariate, the model predicted extant sensory ecology with 92%

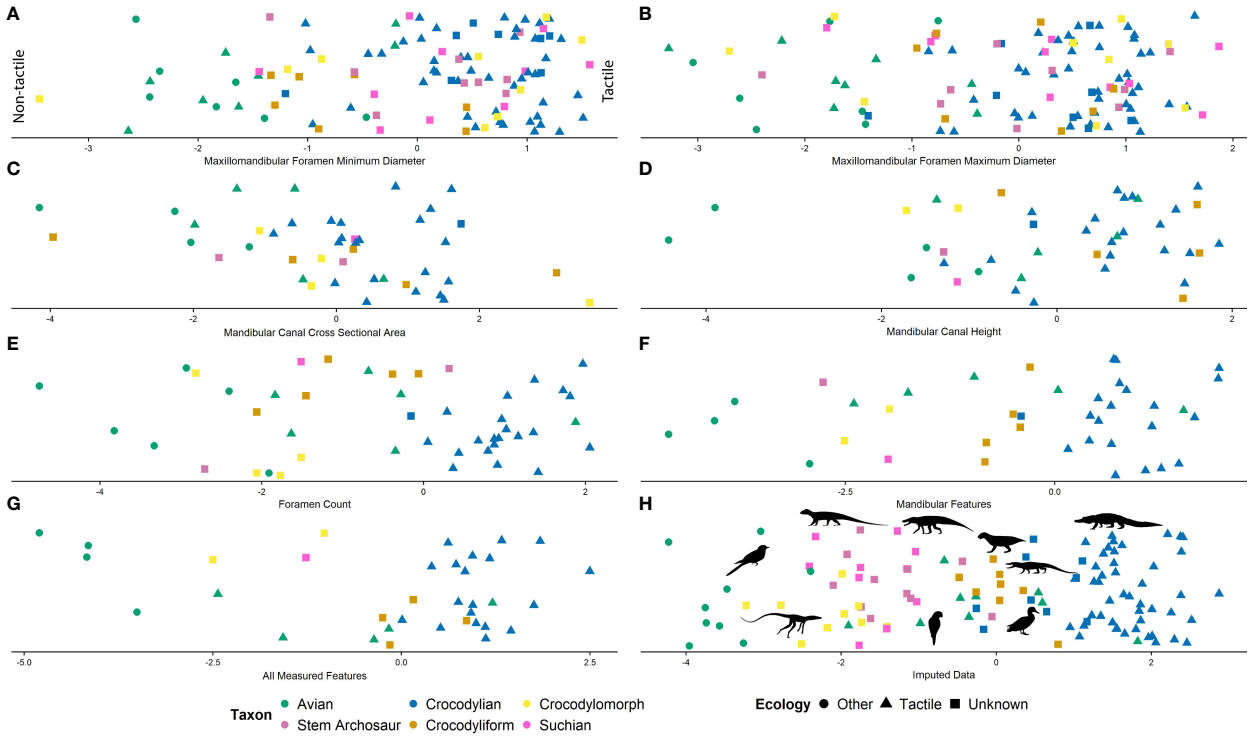

FIGURE 7
Linear discriminant analysis used for ecological predictions for fossil taxa based on **(A)** minimum diameter of the maxillomandibular foramen, **(B)** maximum diameter of the maxillomandibular foramen, **(C)** cross-sectional area of the mandibular canal, **(D)** height of the mandibular canal, **(E)** foramen count, **(F)** all mandibular features, **(G)** all metrics, and **(H)** imputed data.

accuracy, with only *Psittacus* (MUVC AV092), *Fulica* (MUVC AV285), *Phasianus* (MUVC AV263), *Phoebastria* (OUVC 10905), and *Scolopax* (USNM 292760) predicted to be opposite as classified (Figure 7B). For the minimum diameter of the maxillomandibular foramen and foramen magnum width as a covariate, the model predicted extant sensory ecology with 90% accuracy, with only *Psittacus* (MUVC AV092), *Pandion* (MUVC AV335), *Fulica* (MUVC AV285), *Phoebastria* (OUVC 10905), *Scolopax* (USNM 292760), and *Arenaria* (USNM 612977) predicted to be opposite as classified (Figure 7A). The model of the cross-sectional area of the mandibular canal with dentary surface area as a covariate predicted extant sensory ecology with 93% accuracy, with only *Psittacus* (MUVC AV092) and *Fulica* (MUVC AV285) predicted to be opposite as classified (Figure 7C). A model using height of the mandibular canal and dentary surface area as a covariate predicted extant sensory ecology with 94% accuracy, with only *Megascops* (MUVC AV073) and *Fulica* (MUVC AV285) predicted to be opposite as classified (Figure 7D). A final model using foramen count and dentary surface area as a covariate predicted extant sensory ecology with 94% accuracy, with only *Psittacus* (MUVC AV092) and *Arenaria* (USNM 612977) predicted to be opposite as classified (Figure 7E). All predictions for fossil specimens are listed in Supplementary File S1.

Missing data was imputed and the dataset re-evaluated using the model, including all metrics, broadening the sample to 84 extant and 68 fossil specimens. The model predicted extant sensory ecology with 98% accuracy, with only *Psittacus* (MUVC AV092) predicted to be opposite as classified (Figure 7H). All predictions for fossil specimens are listed in Supplementary File S1.

Among the extinct specimens, the imputed data is consistent in predicting the stem archosaur *Trilophosaurus* as non-tactile. Members of Phytosauria and Aetosauria were predicted as tactile. Non-crocodyliform crocodylomorphs were largely predicted as tactile in all models except for *Litargosuchus*, *Junggarsuchus*, and *Macelognathus*. Among the non-crocodylian crocodyliforms sampled, *Protosuchus* and *Nominosuchus* are the only taxa in which the models result in non-tactile predictions (Supplementary File S1).

3.6 Relative size of osteological correlates

Means of osteological correlates (e.g., minimum and maximum maxillomandibular foramen diameter vs. foramen magnum width, and foramen count, mandibular foramen height, and mandibular foramen cross-sectional area vs. dentary surface area) among phylogenetically grouped taxa (e.g., lepidosaurs, non-archosaurian archosauromorphs phytosaurs, aetosaurs, non-crocodylomorph suchians, non-crocodyliform crocodylomorphs, non-crocodylian crocodyliforms, and avians) were compared using phylogenetic ANOVAs with size proxies included as covariates. Though there was no significant difference between group means, some patterns were evident in the data (Figure 8; Supplementary File S1).

Relative maxillomandibular foramen size is largest in extant crocodylians. Lepidosaurs and suchians excluding non-

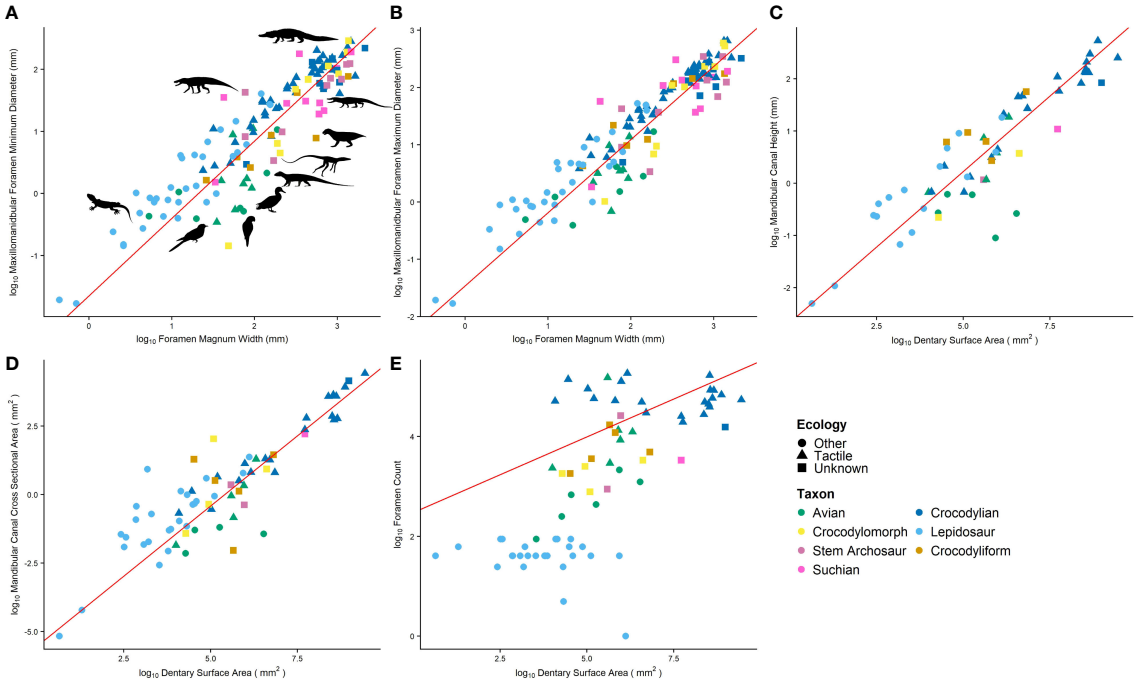

FIGURE 8
Relative sizes of cranial osteological correlates including **(A)** minimum and **(B)** maximum diameter of the maxillomandibular foramen, mandibular canal **(C)** cross-sectional area and **(D)** height, and **(E)** foramen count. Red regression in line is calculated by phylogenetic RMA regression and models the average of tactile taxa.

crocodyliform crocodylomorphs share a similar mean. Non-crocodyliform crocodylomorphs and avians share the smallest means. Relative mandibular canal cross-sectional area is smallest in avians, and all other taxa have similar means. Relative mandibular canal height is largest in crocodyliforms, and avians have some of the smallest canals. Archosauromorphs, aetosaurs, and crocodylomorphs have intermediate-sized canals. Relative foramen counts increase along the pseudosuchian line to extant crocodylians. Tactile avian relative foramen counts are comparable to crocodylians, and non-tactile avians and lepidosaur taxa have the lowest relative foramen counts. Tactile taxa have greater means than non-tactile taxa for all metrics (Figure 8; Supplementary File S1).

4 Discussion

4.1 Morphology

4.1.1 Lateral braincase wall

The specimens observed here do not vary significantly from discussions of lateral braincase wall evolution detailed elsewhere (e.g., Holliday, 2006; Holliday and Witmer, 2009), and therefore there is no further discussion here.

4.1.2 Dentary

In general, foramina or trigeminal neurovasculature distribution in dorsoventrally tall mandibles tends to occur along the alveolar margin (sometimes in a groove) and along the ventral dentary margin. When mandibles are dorsoventrally compressed and more spatulate in shape, (e.g., phytosaurs, crocodylians), there is often a rostral concentration of foramina. In the theropod taxa with mediolaterally compressed mandibles, the mandibular canal is located ventral to the alveoli rather than ventrolateral as in the pseudosuchian taxa, and the neurovascular morphology may differ as a result of alveolar depth (Bouabdellah et al., 2022). Additionally, in taxa with mediolaterally narrow, elongate mandibles (e.g., *Laganosuchus*, thalattosuchians, *Elosuchus*), there is a reduction in foramina numbers. These taxa are secondarily aquatic, and we hypothesize that this reduction occurs as a result of morphological constraint. The same pattern is not observed when comparing longirostrine (e.g., *Gavialis* and *Tomistoma*) and brevirostrine crocodylians (e.g., *Caiman* and *Alligator*), which both exhibit high foramina counts and densities. Whereas a reduction in foramina is present in some taxa, notosuchian crocodyliforms have an increase in foramina. Whether this is an independent origin of foraminiferous mandibles from the condition in extant crocodylians or marks the phylogenetic origin of foraminiferous mandibles among suchians is unknown. The latter would be the case if the presence of few foramina in *Elosuchus* is a secondary reduction.

There are some similarities in osteological correlates between taxa believed or known to have keratinous structures in addition to the bony mandible (e.g., Knutsen, 2007; Holliday and Nesbitt, 2013). Distinct foramina accompany the keratinous rhamphotheca on the dentary of birds and turtles, notably the large rostral foramina in many birds, and the row of foramina along the tomial edge in turtles. In extant birds, many of these rostral neurovascular foramina are present at oblique angles (Hieronymus et al., 2009; Lessner et al., 2023a). In extinct suchian taxa with edentulous portions of the

dentary (e.g., aetosaurs, *Macelognathus*), the edentulous portion is often accompanied by more, larger, and groove-like foramina. This rostral portion of the aetosaur mandible has been hypothesized to have a keratinous covering and the foramina passages for vasculature to supply keratin (Parrish, 1994; Demir and Özsemir, 2021).

We propose the use of foramen density as a phylogenetic character in future analysis. Though the taxonomic status of the suchian MCZ 4453 is unknown, the high density of foramina supports its postulated position within Eusuchia (Turner and Pritchard, 2015).

4.2 Osteological correlates

The strength of the correlations indicates that most of the trigeminal osteological features (i.e., trigeminal foramen diameter, mandibular canal cross-sectional area, mandibular canal height) are suitable correlates for their soft-tissue counterparts (i.e., trigeminal ganglion volume, mandibular nerve cross-sectional area, mandibular nerve height). The exception is the count of foramina on the dentary, which does not correlate well with any measured soft tissue feature. The strength of correlations among clades and ecological categories indicates that these patterns occur independent of phylogeny and ecology. Therefore, all osteological features noted, except for foramen counts, may be used for direct predictions of soft tissues in bony and fossil taxa.

4.3 Size proxy and other limitations

One drawback of incomplete or damaged fossil material is that we often lack a good-sized proxy, which is necessary for comparing relative sizes, and therefore implications of the data are often obscured. It is unclear whether the proxies for size used here (i.e., foramen magnum width, dentary surface area) are suitable for such a large sample. There is a general trend of increasing skull size with increasing foramen magnum size and dentary surface area, and using these features did allow for an increased sample size and use of incomplete specimens. Because many fossil specimens are incomplete, we felt it useful to use commonly present features as proxies for size. However, foramen magnum width likely varies widely based on numerous neural and biomechanical constraints, and dentary surface area similarly varies with head shape and other features. For this reason, conservative statistical approaches (e.g., phylogenetic RMA regression) were used when relying on these features was necessary. Further assessment of foramen magnum dimensions and dentary morphologies among vertebrates may discount or support the use of these measurements.

We also recognize that the braincase wall is variable in structure among sauropsids, and thus osteological correlates vary in soft tissue contents. We measured the maxillomandibular foramen in taxa as a proxy for trigeminal ganglion size. Among sauropsids, the ophthalmic division is variable in its exit from the braincase, and therefore its contribution was included in some taxa measured here and ignored in others. Because trigeminal ganglion volume and the diameter of the prootic notch (lepidosaurs) and maxillomandibular foramen (archosaurs) were well correlated with trigeminal ganglion size, we were confident in excluding the ophthalmic measurements. This feature is often small, unprepared, and difficult to measure in fossil specimens as well.

4.4 Differences among ecologies

Though no significant differences were found among ecologies when including lepidosaurs in the sample (Figures 6A–E), differences were significant among archosaurs (Figures 6F–J). This is likely a result of weaknesses introduced by the size proxy used or the limited understanding of lepidosaurian ecologies. Regardless, the means of all trigeminal osteological correlates were larger in taxa engaging in tactile sensory behaviors. Since these osteological features correlate well with their soft tissue counterparts, it is apparent that trigeminal-innervated tactile sensation is dependent on more trigeminal tissues and the increased size of morphologically related bony structures.

Though no trigeminal soft tissue features were found to correlate with foramen counts, here we note a distinct difference in foramen density between taxa engaging in tactile behavior and those that are not. Rostral foramen counts are commonly used without scientific support to predict sensory abilities in fossil taxa (e.g., Ibrahim et al., 2014; Barker et al., 2017; Carr et al., 2017; Rothschild and Naples, 2017; Cerroni et al., 2020; Kawabe and Hattori, 2021). However, we demonstrate that using this feature to predict sensory ecology is only appropriate when size is controlled and the density of foramina is rigorously assessed (Figure 6J).

4.5 Predictions

Of the extant archosaurs, crocodylians were consistently predicted to have the trigeminal tissues for tactile sensation, and only a few avian species were predicted to be opposite as per our categorization. Though parrots have been noted to possess a highly innervated rostral bill tip (Goujon, 1869; Menzel and Lüdicke, 1974; Lessner et al., 2023b), and thus we categorized them as tactile, models consistently indicate that their morphology was more representative of the non-tactile ecology. We posit that this prediction results from the presence of a high concentration of innervation solely on the rostral tomia rather than a widely distributed bill tip organ as in probe- and tactile-foraging birds (Cunningham et al., 2010). Similarly, *Fulica* is consistently predicted as tactile despite our non-tactile classification. The non-tactile classification was chosen because there is little indication in the literature of specialized tactile sensory behaviors in coots. This is an interesting case because feeding convergence is present between coots, dabbling ducks, and other waterfowl (Allouche and Tamisier, 1984). Ducks and geese exhibit a highly innervated rostral bill tip organ used for the tactile discrimination of food (Gottschaldt and Lausmann, 1974; Berkhoudt, 1980), and our data indicates that there is a sensory system convergence between ducks and *Fulica* in addition to the known feeding convergence (Lind and Poulsen, 1963).

The non-tactile prediction for the stem-archosaur indicates that the basal archosaurian condition was one lacking enhanced

trigeminal sensory abilities. Among pseudosuchians, the tactile prediction for phytosaurs is in line with their occupation of semi-aquatic habitats and predictions of enhanced trigeminal sensation in the clade (Lessner and Stocker, 2017). The non-crocodylomorph suchians largely included aetosaurs, which were predicted as tactile. Aetosaurs exhibit relatively larger trigeminal foramina than other suchians (Paes Neto et al., 2021; von Baczko et al., 2022). As discussed above, the rostral, edentulous portion of the aetosaur mandible may have had a keratinous covering, and therefore the enlarged rostral trigeminal features may be a result of the need to extend more vasculature to nourish the growing keratin rather than to provide nervous tissue to the jaws (Demir and Özsemir, 2021). These data reveal a trend of increasing tactile sensory ability along the line to extant crocodylians similar to that described by Lessner et al. (2023a). The non-tactile predictions among the non-crocodyliform crocodylomorphs *Litargosuchus*, *Junggarsuchus*, and *Macelognathus* and the non-crocodylian crocodyliforms *Nominosuchus* and *Protosuchus* indicate that the transition occurred among early-branching crocodyliforms, diverging in the Late Triassic, and preceding the Neosuchian transition to a semi-aquatic ecology [see Lessner et al. (2023a) for divergence dates and other details; Figure 9]. Maxillomandibular foramen diameters resulted in predictions of tactile ecologies for most taxa and therefore are not as informative as hoped.

4.6 Relative size of osteological correlates

Though not statistically significantly different, the trends appearing upon the comparison of relative sizes of osteological correlates generally match the model predictions. The models indicate an increase in tactile sensory abilities present along the crocodylian line, and the maxillomandibular foramen diameter, mandibular canal cross-sectional area, and foramen count all increase from non-crocodyliform

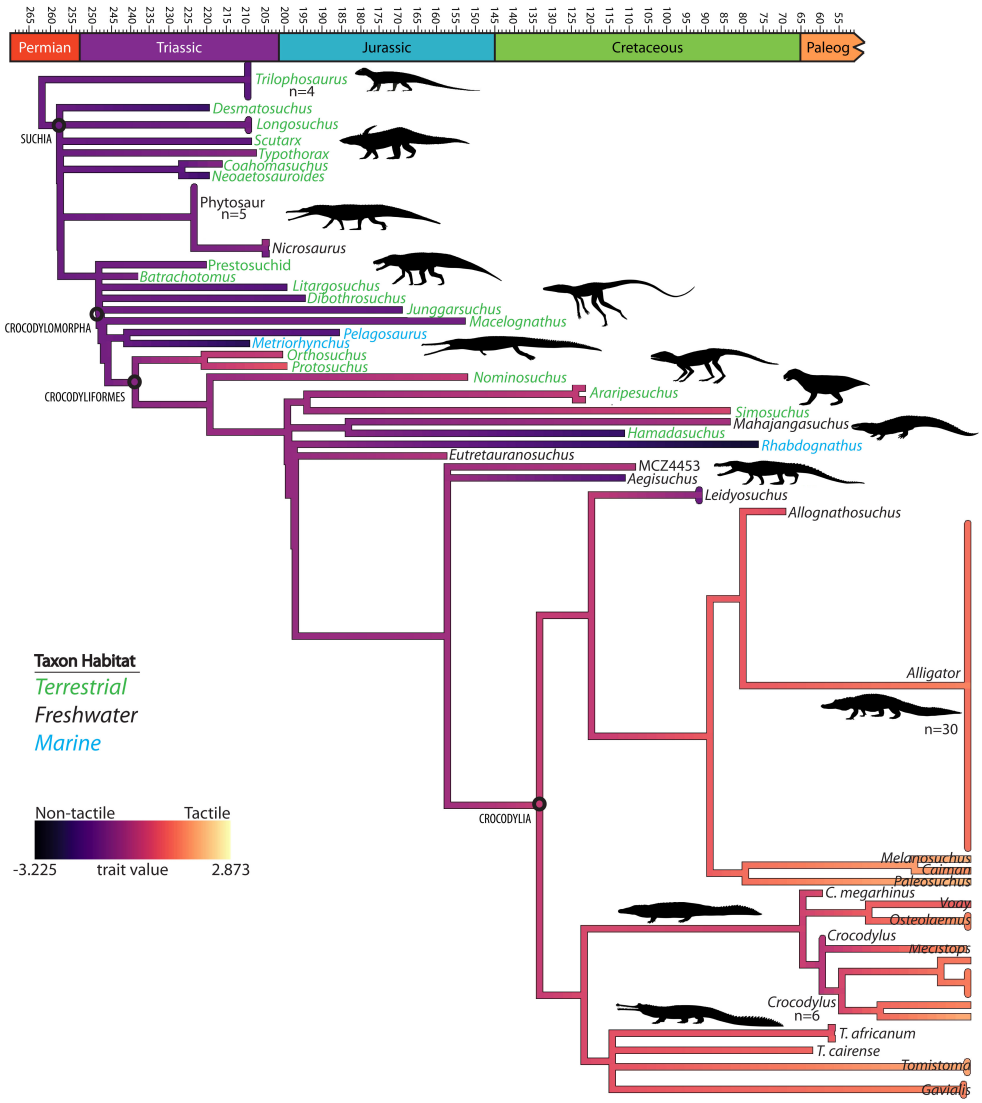

FIGURE 9
Phylogenetic tree of suchian taxa showing a stepwise increase of enhanced tactile sensation with tree branch colors generated from linear discriminant analysis-defined axis for imputed data for all metrics and taxon colors representing habitat.

crocodylomorphs to extant crocodylians (Figures 7–9). There is some variation among basal pseudosuchians, which may be because of the potential semi-aquatic specialization of the phytosaur trigeminal system and beak innervation in aetosaurs.

Lepidosaurs are expected to have small relative features, but generally do not (Figures 6, 8; Supplementary File S1). Both the degree of variation and the high average in lepidosaur maxillomandibular foramen diameters indicate that the foramen magnum width may not be a suitable size proxy. These measurements may also be artificially inflated because of the lack of complete bony bounds for the trigeminal ganglion and divisions. Therefore, measuring the prootic notch in the absence of soft tissue may be an overestimate of trigeminal tissue size. Additionally, little is known about relative sensitivity among lepidosaurs; therefore, it is possible that the non-tactile designations assigned in the analysis are not accurate and lepidosaurs retain large trigeminal nervous tissues for increased tactile abilities.

The degree of variation and the inconsistent averages in avians indicate similar issues. Beak shape is highly variable (e.g., Cooney et al., 2017) and thus may confound surface area measurements (Figures 8C–E). Regardless, tactile taxa consistently exhibit larger osteological correlates with respect to the mandible but not with respect to the braincase (Figure 8; Supplementary Figure S1). The avian braincase is relatively large and takes up most of the skull (Balanoff et al., 2013), leaving little room for other tissues. Therefore, foramina and canals are often exactly the size of their contents and direct osteological correlates for neurovasculature. For this reason, we suspect that the maxillomandibular foramen size in avians may underestimate trigeminal ganglion size as the intracranial ganglion can be substantially larger than the nerve divisions. Often, trigeminal ganglia leave an impression in the avian braincase, and this feature may be more useful for comparison.

5 Conclusions

Overall, the osteology associated with the trigeminal sensory system is quite variable among sauropsids. In spite of this variation, statistically supported predictions of somatosensory abilities are still possible, and this data, in addition to data from Lessner et al. (2023a), supports evolutionary trends within pseudosuchians (Figure 9). Though other conclusions are limited, this reveals a number of interesting avenues worth pursuing, including broad proxies for body size, relative sensitivities and ecologies of lepidosaurs, and use of osteological correlates as phylogenetic characters. Further quantification of additional osteological correlates among clades and ecologies will help inform inferences of behavior in extinct animals and contribute to a complete picture of vertebrate sensory evolution.

Data availability statement

The original contributions presented in the study are included in the article/Supplementary Material. Further inquiries can be directed to the corresponding author.

Ethics statement

Ethical approval was not required for the study involving animals in accordance with the local legislation and institutional requirements because animals were deceased before acquisition.

Author contributions

EL: Conceptualization, Data curation, Formal analysis, Investigation, Methodology, Visualization, Writing – original draft, Writing – review & editing. XX: Resources, Writing – review & editing. BY: Resources, Writing – review & editing. ME: Resources, Writing – review & editing. MJ: Resources, Writing – review & editing. RE: Resources, Writing – review & editing. CH: Conceptualization, Funding acquisition, Investigation, Methodology, Resources, Software, Supervision, Visualization, Writing – review & editing.

Funding

The author(s) declare financial support was received for the research, authorship, and/or publication of this article. This study was supported by National Science Foundation Division of Earth Sciences (NSF EAR 1631684, 1762458; to CH) and Division of Integrative Organismal Biology (NSF IOS 1457319; to CH), Missouri Research Board (to CH), Evolving Earth Foundation (to EJL), Jurassic Foundation (to EJL), Society of Vertebrate Paleontology (to EL), University of Missouri Life Sciences Fellowship Program (to EL), Department of Pathology and Anatomical Sciences, University of Missouri School of Medicine, American Ornithological Society (to EL), Animal Behavior Society (to EL), American Association for Anatomy (to EJL), Society for Integrative and Comparative Biology (to EL), Geological Society of America (to EL), Paleontological Society (to EL), National Natural Science Foundation of China (42288201; to XX), Yunnan Revitalization Talent Support Program (202305AB350006; to XX), and Australian Synchotron (162/IM/10666 and 172/IMBL/11997; to MJ).

Acknowledgments

We thank K. Middleton, A. Lawrence, and H. Petermann for advice on statistical analysis and T. Swift for discussion. Thanks to T. Selley, J. Schiffbauer, and MizzoμX and J. Maisano, M. Colbert, D. Edey and UTCT; University of Missouri Imaging Services staff for CT scanning. Thanks to University of Texas Vertebrate Collections and M. Brown, C. Sagebiel, and K. Bader; the Florida Keys Wild Bird Rehabilitation Center; the FMNH and A. Resetar; Utah Museum of Natural History and K. Melstrom, N. Ong, R. Irmis, C. Levitt-Bussian, and T. Birthisel; the South Australian Museum and M. Hutchinson; Harvard University Museum of Comparative Zoology and C. Byrd and S. Pierce; Stuttgart State Museum of Natural History and R. Schoch; Petrified Forest National Park and M. Smith; Denver Museum of Nature and

Science; and K. Mackenzie and J. Sertich for specimen access. Additional thanks to Morphosource, Digimorph, J. Clarke, L. Jacobs, J. Choiniere, M. Norrell, G. Bever, A. Balanoff, P. Sereno, N. Kley, A. Turner, P. O'Connor, and T. Adams for data sharing and transfer. We acknowledge NSF grants IIS-9874781, IIS-0531767, EAR-0617561, EAR-0854218, and EAR-1525915 for shared data.

Conflict of interest

The authors declare that the research was conducted in the absence of any commercial or financial relationships that could be construed as a potential conflict of interest.

Publisher's note

All claims expressed in this article are solely those of the authors and do not necessarily represent those of their affiliated organizations, or those of the publisher, the editors and the reviewers. Any product that may be evaluated in this article, or claim that may be made by its manufacturer, is not guaranteed or endorsed by the publisher.

Author disclaimer

The conclusions presented here are those of the authors and do not represent the views of the United States Government.

Supplementary material

The Supplementary Material for this article can be found online at: https://www.frontiersin.org/articles/10.3389/famrs.2024.1411516/full#supplementary-material

SUPPLEMENTARY FIGURE 1
Residuals of cranial osteological correlates including **(A)** minimum and **(B)** maximum diameter of the maxillomandibular foramen, mandibular canal **(C)** cross-sectional area and **(D)** height, and **(E)** foramen count.

References

Abdel-Kader, T. G., Ali, R. S., and Ibrahim, N. M. (2011). The cranial nerves of *Mabuya quinquetaeniata* III: nervus trigeminus. *Life Sci. J.* 8, 650–669.

Allouche, L., and Tamisier, A. (1984). Feeding convergence of Gadwall, Coot and the other herbivorous waterfowl species wintering in the Camargue: a preliminary approach. *Wildfowl* 35, 135–142.

Balanoff, A. M., Bever, G. S., and Ikejiri, T. (2010). The braincase of *Apatosaurus* (Dinosauria: Sauropoda) based on computed tomography of a new specimen with comments on variation and evolution in sauropod neuroanatomy. *Am. Mus. Novit.* 2010, 1–32. doi: 10.1206/591.1

Balanoff, A. M., Bever, G. S., Rowe, T. B., and Norell, M. A. (2013). Evolutionary origins of the avian brain. *Nature* 501, 93–96. doi: 10.1038/nature12424

Barbas-Henry, H. A., and Lohman, A. H. (1986). The motor complex and primary projections of the trigeminal nerve in the monitor lizard, *Varanus exanthematicus*. *J. Comp. Neurol.* 254, 314–329. doi: 10.1002/cne.902540305

Barker, C. T., Naish, D., Newham, E., Katsamenis, O. L., and Dyke, G. (2017). Complex neuroanatomy in the rostrum of the Isle of Wight theropod *Neovenator salerii*. *Sci. Rep.* 7, 1–8. doi: 10.1038/s41598-017-03671-3

Baumel, J. J., and Witmer, L. M. (1993). "Osteologia," in *Handbook of Avian Anatomy Nomina Anatomica Avium, 2nd Edition*. Eds. J. J. Baumel, A. S. King, J. E. Breazile, H. E. Evans and J. C. Vanden Berge (Cambridge: Nuttall Ornithological Society), 45–131.

Berkhoudt, H. (1980). The morphology and distribution of cutaneous mechanoreceptors (Herbst and Grandy corpuscules) in bill and tongue of the mallard (*Anas platyrhynchos*). *Neth. J. Zool.* 30, 1–34. doi: 10.1163/002829680X00014

Bird, D. J., Amirkhanian, A., Pang, B., and Van Valkenburgh, B. (2014). Quantifying the cribriform plate: influences of allometry, function, and phylogeny in Carnivora. *Anat. Rec.* 297, 2080–2092. doi: 10.1002/ar.23032

Bird, D. J., Murphy, W. J., Fox-Rosales, L., Hamid, I., Eagle, R. A., and Van Valkenburgh, B. (2018). Olfaction written in bone: cribriform plate size parallels olfactory receptor gene repertoires in Mammalia. *Proc. R. Soc B. Biol. Sci.* 285, 20180100. doi: 10.1098/rspb.2018.0100

Bouabdellah, F., Lessner, E. J., and Benoit, J. (2022). The rostral neurovascular system of *Tyrannosaurus rex*. *Palaeontol. Electron* 25, 1–21. doi: 10.26879/1178

Carr, T. D., Varricchio, D. J., Sedlmayr, J. C., Roberts, E. M., and Moore, J. R. (2017). A new tyrannosaur with evidence for anagenesis and crocodile-like facial sensory system. *Sci. Rep.* 7, 1–11. doi: 10.1038/srep44942

Catania, K. C., Leitch, D. B., and Gauthier, D. (2010). Function of the appendages in tentacled snakes (*Erpeton tentaculatus*). *J. Exp. Biol.* 213, 359–367. doi: 10.1242/jeb.039685

Cerroni, M. A., Canale, J. I., Novas, F. E., and Paulina-Carabajal, A. (2020). An exceptional neurovascular system in abelisaurid theropod skull: New evidence from *Skorpiovenator bustingorryi*. *J. Anat.* 240, 612–626. doi: 10.1111/joa.13258

Cooney, C. R., Bright, J. A., Capp, E. J., Chira, A. M., Hughes, E. C., Moody, C. J., et al. (2017). Mega-evolutionary dynamics of the adaptive radiation of birds. *Nature* 542, 344–347. doi: 10.1038/nature21074

Crowe-Riddell, J. M., Williams, R., Chapuis, L., and Sanders, K. L. (2019). Ultrastructural evidence of a mechanosensory function of scale organs (sensilla) in sea snakes (Hydrophiinae). *R. Soc Open Sci.* 6, 182022. doi: 10.1098/rsos.182022

Cull, G., Cioffi, G. A., Dong, J., Homer, L., and Wang, L. (2003). Estimating normal optic nerve axon numbers in non-human primate eyes. *J. Glaucoma* 12, 301–306. doi: 10.1097/00061198-200308000-00003

Cunningham, S. J., Alley, M. R., Castro, I., Potter, M. A., Cunningham, M., and Pyne, M. J. (2010). Bill morphology of ibises suggests a remote-tactile sensory system for prey detection. *Auk* 127, 308–316. doi: 10.1525/auk.2009.09117

Cunningham, S. J., Corfield, J. R., Iwaniuk, A. N., Castro, I., Alley, M. R., Birkhead, T. R., et al. (2013). The anatomy of the bill tip of kiwi and associated somatosensory regions of the brain: comparisons with shorebirds. *PloS One* 8, e80036. doi: 10.1371/journal.pone.0080036

Dehnhardt, G., and Kaminski, A. (1995). Sensitivity of the mystacial vibrissae of harbour seals (*Phoca vitulina*) for size differences of actively touched objects. *J. Exp. Biol.* 198, 2317–2323. doi: 10.1242/jeb.198.11.2317

Demir, A., and Özsemir, K. G. (2021). Retrospective study of beak deformities in birds. *Turk. Vet. J.* 3, 13–20. doi: 10.51755/turkvetj.819479

Di-Poï, N., and Milinkovitch, M. C. (2013). Crocodylians evolved scattered multi-sensory micro-organs. *EvoDevo* 4, 1–19. doi: 10.1186/2041-9139-4-19

Dollman, K. N. (2020). Biostratigraphy, systematics, taxonomy and palate evolution in early branching southern African crocodylomorphs. Johannesburg, South Africa: University of the Witwatersrand.

Evans, S. E. (2008). The skull of lizards and tuatara. *Biol. Reptilia* 20, 1–347.

George, I. D., and Holliday, C. M. (2013). Trigeminal nerve morphology in *Alligator mississippiensis* and its significance for crocodyliform facial sensation and evolution. *Anat. Rec.* 296, 670–680. doi: 10.1002/ar.22666

Gignac, P. M., Kley, N. J., Clarke, J. A., Colbert, M. W., Morhardt, A. C., Cerio, D., et al. (2016). Diffusible iodine-based contrast-enhanced computed tomography (diceCT): an emerging tool for rapid, high-resolution, 3-D imaging of metazoan soft tissues. *J. Anat.* 228, 889–909. doi: 10.1111/joa.12449

Goris, R. C. (2011). Infrared organs of snakes: an integral part of vision. *J. Herpetol.* 45, 2–15. doi: 10.1670/10-238.1

Gottschaldt, K. M., and Lausmann, S. (1974). The peripheral morphological basis of tactile sensibility in the beak of geese. *Cell Tissue Res.* 153, 477–496. doi: 10.1007/BF00231542

Goujon, D. (1869). Sur un appareil de corpuscules tactiles situe dans le bec des perroquets. *J. L'Anat. la Physiol.* 6, 449–455.

Grap, N. J., Machts, T., Essert, S., and Bleckmann, H. (2020). Stimulus discrimination and surface wave source localization in Crocodilians. *Zool* 139, 125743. doi: 10.1016/j.zool.2020.125743

Hieronymus, T. L., Witmer, L. M., Tanke, D. H., and Currie, P. J. (2009). The facial integument of centrosaurine ceratopsids: morphological and histological correlates of novel skin structures. *Anat. Rec.* 292, 1370–1396. doi: 10.1002/ar.20985

Hiller, U. (1978). Morphology and electrophysiological properties of cutaneous sensilla in agamid lizards. *Pflügers archiv* 377, 189–191. doi: 10.1007/BF00582851

Holliday, C. M. (2006). Evolution and function of the jaw musculature and adductor chamber of archosaurs (crocodilians, dinosaurs, and birds). Athens, Ohio, USA: Ohio University.

Holliday, C. M. (2009). New insights into dinosaur jaw muscle anatomy. *Anat. Rec.* 292, 1246–1265. doi: 10.1002/ar.20982

Holliday, C. M., and Nesbitt, S. J. (2013). Morphology and diversity of the mandibular symphysis of archosauriforms. *Geol. Soc Spec. Publ.* 379, 555–571. doi: 10.1144/SP379.2

Holliday, C. M., and Witmer, L. M. (2007). Archosaur adductor chamber evolution: integration of musculoskeletal and topological criteria in jaw muscle homology. *J. Morphol.* 268, 457–484. doi: 10.1002/jmor.10524

Holliday, C. M., and Witmer, L. M. (2009). The epipterygoid of crocodyliforms and its significance for the evolution of the orbitotemporal region of eusuchians. *J. Vertebr. Paleontol.* 29, 715–733. doi: 10.1671/039.029.0330

Hopson, J. A. (1979). Paleoneurology. *Biol. Reptilia* 9, 39–148.

Hurlburt, G. (1999). Comparison of body mass estimation techniques, using recent reptiles and the pelycosaur *Edaphosaurus boanerges*. *J. Vertebr. Paleontol.* 19, 338–350. doi: 10.1080/02724634.1999.10011145

Ibrahim, N., Sereno, P. C., Dal Sasso, C., Maganuco, S., Fabbri, M., Martill, D. M., et al. (2014). Semiaquatic adaptations in a giant predatory dinosaur. *Science* 345, 1613–1616. doi: 10.1126/science.1258750

Iwaniuk, A. N., Olson, S. L., and James, H. F. (2009). Extraordinary cranial specialization in a new genus of extinct duck (Aves: Anseriformes) from Kauai, Hawaiian Islands. *Zootaxa* 2296, 47–67. doi: 10.11646/zootaxa.2296.1

Jollie, M. T. (1962). *Chordate Morphology* (New York: Reinhold Publishing Co). doi: 10.5962/bhl.title.6408

Jonas, J. B., Schmidt, A. M., Müller-Bergh, J. A., Schlötzer-Schrehardt, U. M., and Naumann, G. O. (1992). Human optic nerve fiber count and optic disc size. *Invest. Ophthalmol. Vis. Sci.* 33, 2012–2018.

Kandel, E., Schwartz, J., and Jessell, T. (2000). *Principals of neural science. 4th ed* (New York: McGraw-Hill).

Kawabe, S., and Hattori, S. (2021). Complex neurovascular system in the dentary of *Tyrannosaurus*. *Hist. Biol.* 34, 1–9. doi: 10.1080/08912963.2021.1965137

Knutsen, E. M. (2007). Beak morphology in extant birds with implications on beak morphology in ornithomimids. Master's thesis. University of Oslo, Norway.

Lakjer, T. (1926). *Studien über die Trigeminus-versorgte Kaumuskulatur der Sauropsiden* (Copenhagen, Denmark: CA Reitzel).

Leitch, D. B., and Catania, ,. K. C. (2012). Structure, innervation and response properties of integumentary sensory organs in crocodilians. *J. Exp. Biol.* 215, 4217–4230. doi: 10.1242/jeb.076836

Lessner, E. J. (2021). Quantifying neurovascular canal branching patterns reveals a shared crocodylian arrangement. *J. Morphol.* 282, 185–204. doi: 10.1002/jmor.21295

Lessner, E. J. (2022). Diversity and evolution of the sauropsid trigeminal sensory system. Columbia, Missouri, USA: University of Missouri.

Lessner, E. J., Dollman, K. N., Clark, J. M., Xing, X., and Holliday, C. M. (2023a). Ecomorphological patterns in trigeminal canal branching among sauropsids reveal sensory sensory shift in suchians. *J. Anat.* 242, 927–952. doi: 10.1111/joa.13826

Lessner, E. J., Echols, M. S., Paul-Murphy, J. R., Speer, B. L., and Holliday, C. M. (2023b). Grey parrot (*Psittacus erithacus*) beak papillae and nerves identified using novel 2-D and 3-D imaging modalities. *Am. J. Vet. Res.* 84, 1–7. doi: 10.2460/ajvr.23.03.0059

Lessner, E. J., and Stocker, M. R. (2017). Archosauriform endocranial morphology and osteological evidence for semiaquatic sensory adaptations in phytosaurs. *J. Anat.* 231, 655–664. doi: 10.1111/joa.12668

Lind, H., and Poulsen, H. (1963). On the morphology and behaviour of a hybrid between Goosander and Shelduck (*Mergus merganser* L. x *Tadorna tadorna* L.). *Z. für Tierpsychologie* 20, 558–569. doi: 10.1111/j.1439-0310.1963.tb01174.x

Mackinnon, S. E., and Dellon, A. L. (1995). Fascicular patterns of the hypoglossal nerve. *J. Reconstr. Microsurg.* 11, 195–198. doi: 10.1055/s-2007-1006531

Marino, L. (2007). Cetacean brains: how aquatic are they? *Anat. Rec.* 290, 694–700. doi: 10.1002/ar.20530

Menzel, R., and Lüdicke, M. (1974). Funktionell-anatomische und autoradiographische Untersuchungen am Schnabelhorn von Papageien (Psittaci). *Zool. Jahrb. Abt. Anat. Ontog. Tiere.* 93, 175–218.

Muchlinski, M. N. (2008). The relationship between the infraorbital foramen, infraorbital nerve, and maxillary mechanoreception: Implications for interpreting the paleoecology of fossil mammals based on infraorbital foramen size. *Anat. Rec.* 291, 1221–1226. doi: 10.1002/ar.20742

Nicolelis, M. A., Lin, R. C., and Chapin, J. K. (1997). Neonatal whisker removal reduces the discrimination of tactile stimuli by thalamic ensembles in adult rats. *J. Neurophysiol.* 78, 1691–1706. doi: 10.1152/jn.1997.78.3.1691

Oelrich, T. M. (1956). The anatomy of the head of *Ctenosaura pectinata* (Iguanidae). *Misc. publ. - Mus. Zool. Univ. Mich.* 94, 1–122.

Oelschlager, H., and Oelschlager, H. (2002). *Encyclopedia of marine mammals* (San Diego: Academic Press).

Paes Neto, V. D., Desojo, J. B., Brust, A. C., Ribeiro, A. M., Schultz, C. L., and Soares, M. B. (2021). The first braincase of the basal aetosaur *Aetosauroides scagliai* (Archosauria: Pseudosuchia) from the Upper Triassic of Brazil. *J. Vertebr. Paleontol.* 41, e1928681. doi: 10.1080/02724634.2021.1928681

Pagel, M. (1999). Inferring the historical patterns of biological evolution. *Nature* 401, 877–884. doi: 10.1038/44766

Paradis, E., and Schliep, K. (2019). ape 5.0: an environment for modern phylogenetics and evolutionary analyses in R. *Bioinform.* 35, 526–528. doi: 10.1093/bioinformatics/bty633

Parrish, J. M. (1994). Cranial osteology of *Longosuchus meadei* and the phylogeny and distribution of the Aetosauria. *J. Vertebr. Paleontol.* 14, 196–209. doi: 10.1080/02724634.1994.10011552

Pennell, M., Eastman, J., Slater, G., Brown, J., Uyeda, J., Fitzjohn, R., et al. (2014). geiger v2.0: an expanded suite of methods for fitting macroevolutionary models to phylogenetic trees. *Bioinform.* 30, 2216–2218. doi: 10.1093/bioinformatics/btu181

Pinhiero, J., Bates, D., DebRoy, S., and Sarkar, D. (2013). *nlme: Linear and Nonlinear Mixed Effects Models. R package version 3.1–108*. Available at: https://svn.r-project.org/R-packages/trunk/nlme/.

Poglayen-Neuwall, I. (1953). Untersuchungen der Kiefermuskulatur und deren Innervation an Krokodilen. *Anat. Anz.* 99, 257–296.

R Core Team (2021). *R: A language and environment for statistical computing* (Vienna, Austria: R Foundation for Statistical Computing). Available at: https://www.R-project.org/.

Revell, L. J. (2012). phytools: An R package for phylogenetic comparative biology (and other things). *Methods Ecol. Evol.* 3, 217–223. doi: 10.1111/j.2041-210X.2011.00169.x

Rothschild, B. M., and Naples, V. (2017). Apparent sixth sense in theropod evolution: The making of a Cretaceous weathervane. *PloS One* 12, e0187064. doi: 10.1371/journal.pone.0187064

Schumacher, G. H. (1973). "The head muscles and hyolaryngeal skeleton of turtles and Crocodilians," in *Biology of the Reptilia*, vol. 4 . Eds. C. Gans and T. S. Parsons (Academic Press, London), 101–199.

Smaers, J. B., and Mongle, C. S. (2014). *evomap: R package for the evolutionary mapping of continuous traits* (GitHub). Available at: https://github.com/JeroenSmaers/evomap.

Soares, D. (2002). An ancient sensory organ in crocodilians. *Nature* 417, 241–242. doi: 10.1038/417241a

Turner, A. H., and Pritchard, A. C. (2015). The monophyly of Susisuchidae (Crocodyliformes) and its phylogenetic placement in Neosuchia. *PeerJ* 3, e759. doi: 10.7717/peerj.759

van Buuren, S., and Groothuis-Oudshoorn, K. (2011). mice: multivariate imputation by chained equations in R. *J. Stat. Software* 45, 1–67. doi: 10.18637/jss.v045.i03

Venables, W. N., and Ripley, B. D. (2002). *Modern Applied Statistics with S. 4th ed.* (New York: Springer). Available at: https://www.stats.ox.ac.uk/pub/MASS4/.

von Baczko, M. B., Desojo, J. B., Gower, D. J., Ridgely, R., Bona, P., and Witmer, L. M. (2022). New digital braincase endocasts of two species of *Desmatosuchus* and neurocranial diversity within Aetosauria (Archosauria: Pseudosuchia). *Anat. Rec.* 305, 2415–2434. doi: 10.1002/ar.24798

Watanabe, T., and Yasuda, M. (1970). Comparative and topographical anatomy of the fowl. XXVI. Peripheral course of the trigeminal nerve. *Japan. J. Vet. Sci.* 32, 43–57. doi: 10.1292/jvms1939.32.43

Watkinson, G. B. (1906). The cranial nerves of *Varanus bivittatus*. *Gegenbaurs Morphol. Jahrb.* 35, 450–472.

Witmer, L. M., and Ridgely, R. C. (2009). New insights into the brain, braincase, and ear region of tyrannosaurs (Dinosauria, Theropoda), with implications for sensory organization and behavior. *Anat. Rec.* 292, 1266–1296.

Witmer, L. M., Ridgely, R. C., Dufeau, D. L., and Semones, M. C. (2008). "Using CT to peer into the past: 3D visualization of the brain and ear regions of birds, crocodiles, and nonavian dinosaurs," in *Anatomical imaging*. Eds. H. Endo and R. Frey (Tokyo: Springer), 67–87.

Witmer, L. M., and Thomason, J. J. (1995). The extant phylogenetic bracket and the importance of reconstructing soft tissues in fossils. *Funct. Morphol. Vertebr. Paleontol.* 1, 19–33.

Wylie, D. R., Gutiérrez-Ibáñez, C., and Iwaniuk, A. (2015). Integrating brain, behavior, and phylogeny to understand the evolution of sensory systems in birds. *Front. Neurosci.* 9, 281. doi: 10.3389/fnins.2015.00281

Anatomical abbreviations

b, brain; fV_1, foramen for the ophthalmic division of the trigeminal nerve; $fV_{2/3}$, foramen for the maxillomandibular divisions of the trigeminal nerve; ls, laterosphenoid; n.pr, prootic notch; pr, prootic; q, quadrate; V, trigeminal nerve; V_1, ophthalmic division of the trigeminal nerve; V_2, maxillary division of the trigeminal nerve; V_3, mandibular division of the trigeminal nerve; V_f, trigeminal foramen; V_g, trigeminal ganglion.

Institutional abbreviations

AMNH, American Museum of Natural History, New York, New York, USA; BMNH (NHMUK), British Museum of Natural History, London, England; BP, Bernard Price Institute for Paleontological Research, Johannesburg, South Africa; BRLSI, Bath Royal Literary and Scientific Institution, Bath, England; BYU, Brigham Young University Museum of Paleontology, Provo, Utah, USA; CNRST-SUNY, Centre National de la Recherche Scientifique et Technologique de Mali – Stony Brook University, New York, New York, USA; CUP, Catholic University of Peking, Beijing, China; DINO, Dinosaur National Monument, Jensen, Utah, USA; DMNH, Denver Museum of Nature and Science, Denver, Colorado, USA; FMNH, Field Museum of Natural History, Chicago, Illinois, USA; GR, Ghost Ranch, Abiquiu, New Mexico, USA; IGM, Institute of Geology, Ulaanbaatar, Mongolia; IVPP, Institute of Vertebrate Paleontology and Paleoanthropology, Beijing, China; LACM, Natural History Museum of Los Angeles County, Los Angeles, California, USA; MCZ, Museum of Comparative Zoology, Cambridge, Massachusetts, USA; MNA, Museum of Northern Arizona, Flagstaff, Arizona, USA; MNN, Muséum National du Niger, Niamey, République de Niger; MOR, Museum of the Rockies, Bozeman, Montana, USA; MUO, Museum of the University of Oklahoma, Norman, Oklahoma, USA; MUVC, University of Missouri Vertebrate Collection, Columbia, Missouri, USA; MWC, Museum of the West, Grand Junction, Colorado, USA; OUVC, Ohio University Vertebrate Collection, Athens, Ohio, USA; PEFO, Petrified Forest National Park, Arizona, USA; PVL, Paleontologia de Vertebrados Lillo, Universidad Nacional de Tucumán, Tucumán, Argentina; ROM, Royal Ontario Museum, Toronto, Ontario, Canada; SAM, South African Museum, Cape Town, Western Cape Province, South Africa; SAMA, South Australia Museum, Adelaide, Australia; SMNS, State Museum of Natural History, Stuttgart, Germany; TMM (TNHC), Texas Memorial Museum, Austin, Texas, USA; UA, Université d'Antananarivo, Atntananarivo, Madagascar; UADBA, Université d'Antananarivo, Département de Biologie Animale, Atntananarivo, Madagascar; UALVP, University of Alberta Laboratory for Vertebrate Paleontology, Edmonton, Alberta, Canada; UC, University of Chicago, Chicago, Illinois, USA; UCMP, University of California Museum of Paleontology, Berkeley, California, USA; UCR, Universidade Estadual Paulista, Rio Claro, São Paulo, Brazil; UF, University of Florida, Gainsville, Florida, USA; UMNH (UUVP), Utah Museum of Natural History, Salt Lake City, Utah, USA; USNM, Smithsonian National Museum of Natural History, Washington, DC, USA; YPM, Yale Peabody Museum, New Haven, Connecticut, USA.